AD-A067 711 ALASKA UNIV FAIRBANKS GEOPHYSICAL INST F/G 4/1
INVESTIGATION OF THE PHENOMENOLOGY OF THE ARCTIC IONOSPHERE AND--ETC(U)
SEP 78 S AKASOFU F19628-76-C-0074
UNCLASSIFIED AFGL-TR-78-0269-PT-1 NL

| OF |
ADA
067711

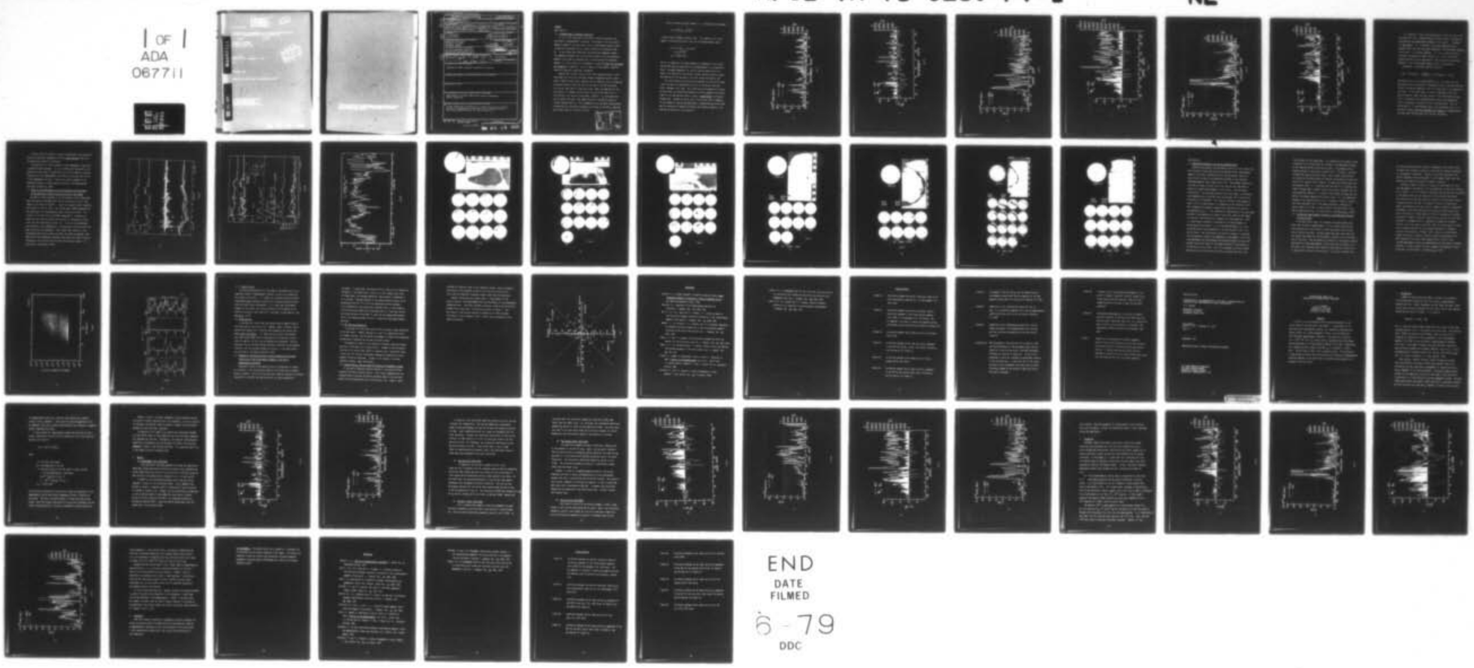

END
DATE
FILMED
6-79
DDC

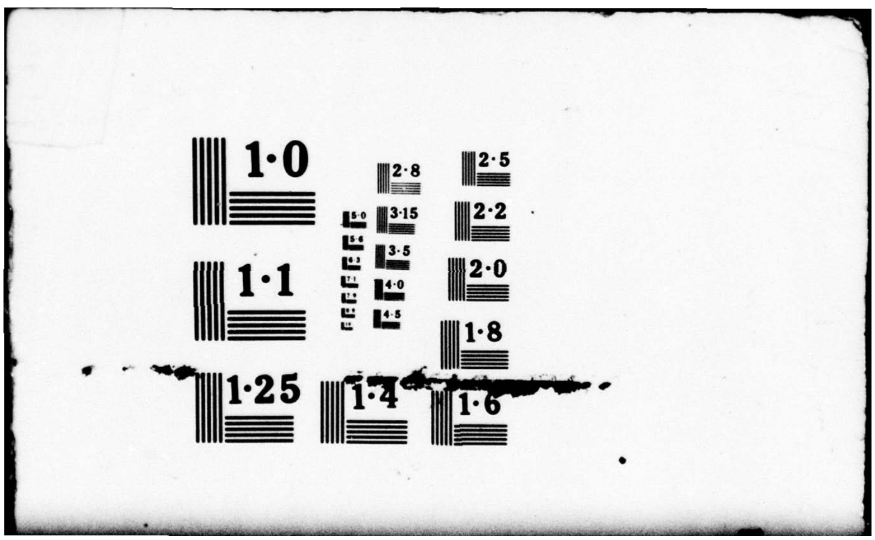
1·0
2·8
2·5
5·0
3·15
2·2
5·6
3·5
1·1
4·0
2·0
4·5
1·8
1·25
1·4
1·6

, ALASKA 99701

port

1, 1975 - September 30, 1976

er, 1976

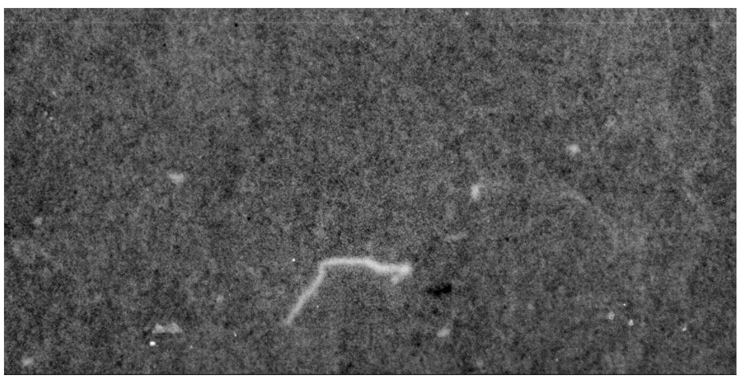

19 **REPORT DOCUMENTATION PAGE**

READ INSTRUCTIONS BEFORE COMPLETING FORM

1. REPORT NUMBER
18 AFGL-TR-78-0269- PT-1

2. GOVT ACCESSION NO.

3. RECIPIENT'S CATALOG NUMBER

4. TITLE (and Subtitle)
6 INVESTIGATION OF THE PHENOMENOLOGY OF THE ARCTIC IONOSPHERE AND ITS RELATION TO THE PHENOMENOLOGY OF ARCTIC PARTICLE PRECIPITATION. Part I.

5. TYPE OF REPORT & PERIOD COVERED
Final Report
October 2, 1975-September 30, 1978

6. PERFORMING ORG. REPORT NUMBER

7. AUTHOR(s)
10 S.-I. Akasofu

8. CONTRACT OR GRANT NUMBER(s)
15 F19628-76-C-0074

9. PERFORMING ORGANIZATION NAME AND ADDRESS
Geophysical Institute
University of Alaska
Fairbanks, Alaska

10. PROGRAM ELEMENT, PROJECT, TASK AREA & WORK UNIT NUMBERS
62101F
16 76630801
17 08

11. CONTROLLING OFFICE NAME AND ADDRESS
Air Force Geophysics Laboratory
Hanscom AFB, Massachusetts 01731
Monitor/Pauline Krukonis/PHI

12. REPORT DATE
11 Sep [redacted] 78

13. NUMBER OF PAGES
62
12 59p.

14. MONITORING AGENCY NAME & ADDRESS (if different from Controlling Office)
9 Final rept. 2 Oct 75-30 Sep 78,

15. SECURITY CLASS. (of this report)
Unclassified

15a. DECLASSIFICATION/DOWNGRADING SCHEDULE

16. DISTRIBUTION STATEMENT (of this Report)

Approved for public release; distribution unlimited

17. DISTRIBUTION STATEMENT (of the abstract entered in Block 20, if different from Report)

18. SUPPLEMENTARY NOTES

19. KEY WORDS (Continue on reverse side if necessary and identify by block number)

Magnetospheric substorm, DMSP auroral scanner photographs, auroral morphology

20. ABSTRACT (Continue on reverse side if necessary and identify by block number)

We have established the possibility of predicting the occurrence and intensity of magnetospheric substorms and also suggested a way of monitoring substorm activity on a real time basis.

152650 mt

79 04 19 030

Summary

Major Results

(i) A breakthrough in substorm prediction

It is of vital importance to the USAF to predict accurately the occurrence of magnetospheric substorms. The success of this task would depend on whether or not one could find an interplanetary quantity which is physically meaningful and is closely related to the substorm index AE. It has already been known that the north-south component (namely, the component perpendicular to the ecliptic plane) of the interplanetary magnetic field plays an important role in the occurrence of substorms. However, it is too crude to be a parameter in predicting both the occurrence and intensity of substorms. For this reason, we have made an intensive search for physically meaningful parameters.

Knowing that the daily sum of the Kp index (denoted by ΣKp) is well correlated with the solar wind speed (Snyder, Neugebauer and Rao, 1963; Olbert, 1968) and that the B_z component has an important role in triggering substorms (Arnoldy, 1971) and that the variance of the IMF correlates with the Kp index (Ballif, Jones and Colman, 1969), we examined also the relationship (i) between the variance of B_z and the AE index and (ii) the variance of B_z and solar wind speed. However, it is concluded that one can hardly say that a high speed variance of the IMF B_z causes an intense substorm activity. This statement can also be easily demonstrated by examining the relationship between the variance of the IMF B_z component and the ΣKp index as a function of time.

After an extensive search, however, it is found that the parameter

$$\varepsilon(t) = VB^2 \left(\ell_0 \sin^2 \frac{\theta'}{2}\right)^2$$

is most closely related to the AE index. This quantity $\varepsilon(t)$ is the amount of Poynting flux which flows into the magnetosphere, where

$$\begin{aligned} \int dS = S &= \{\ell_0(1 - \sin \theta/2)\}^2 \\ &= \{\ell_0 \sin^2 \frac{\theta'}{2}\}^2 \\ \ell_0 &= 7 \text{ earth radii}, \end{aligned}$$

and θ' is a measure of the angle between the geomagnetic field vector and the IMF vector at the front of the magnetosphere in the equatorial plane. The above expression for $\int dS$ was obtained empirically as a result of an effort to find the most suitable expression which relates the Poynting flux to the rate of the total energy dissipation $u(t)$.

This can be seen in the relationship between $\varepsilon(t)$ and the AE index. Figure 1a shows this relationship for one of the typical recurrent storms, November 3-10, 1973. This figure may be contrasted with Figure 1b which shows the relationship between the IMF B_z component and the AE index for the same period; there is hardly a quantitative relationship between them. Figures 2a and 2b, and 3a and 3b show similar examples; for more examples, see the attached paper. Recognizing the the AE index does not necessarily represent accurately the substorm intensity, the obtained correlation is very assuring.

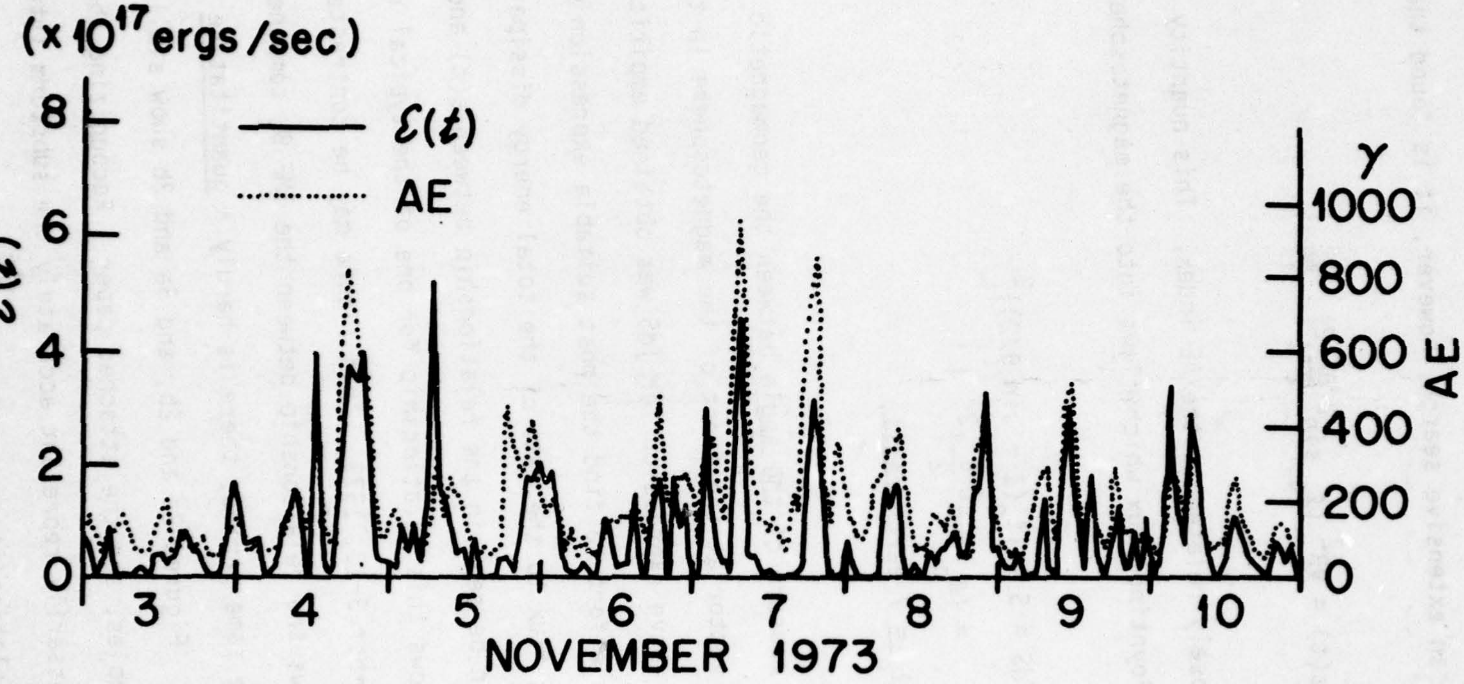

(x 10^{17} ergs/sec)
$\mathcal{E}(t)$
AE
8
6
4
2
0
γ
1000
800
600
400
200
0
AE
3
4
5
6
7
8
9
10
NOVEMBER 1973

Fig 1a

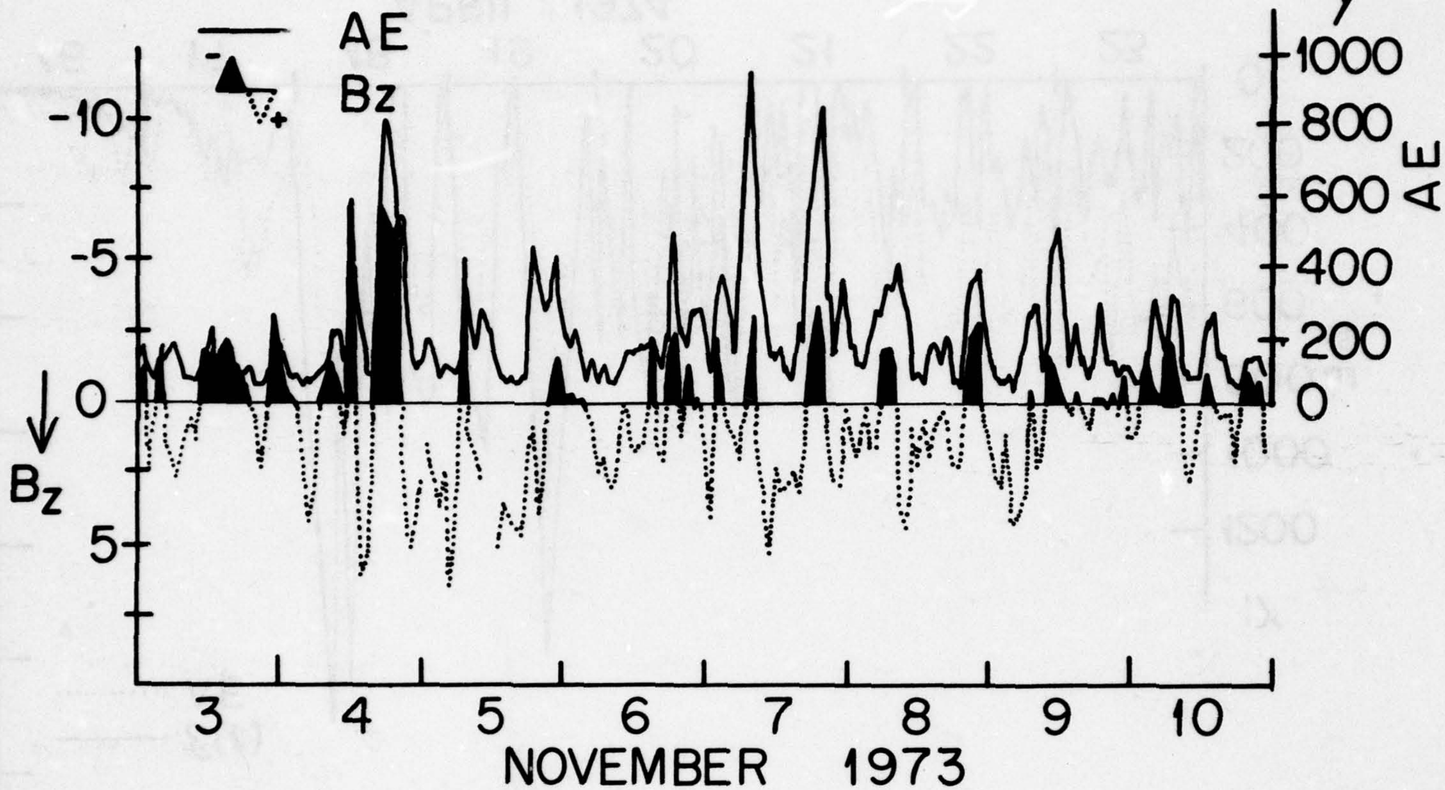
AE
Bz
-10
-5
0
5
Bz
γ
1000
800
600
400
200
0
AE
3
4
5
6
7
8
9
10
NOVEMBER 1973

Fig 1b

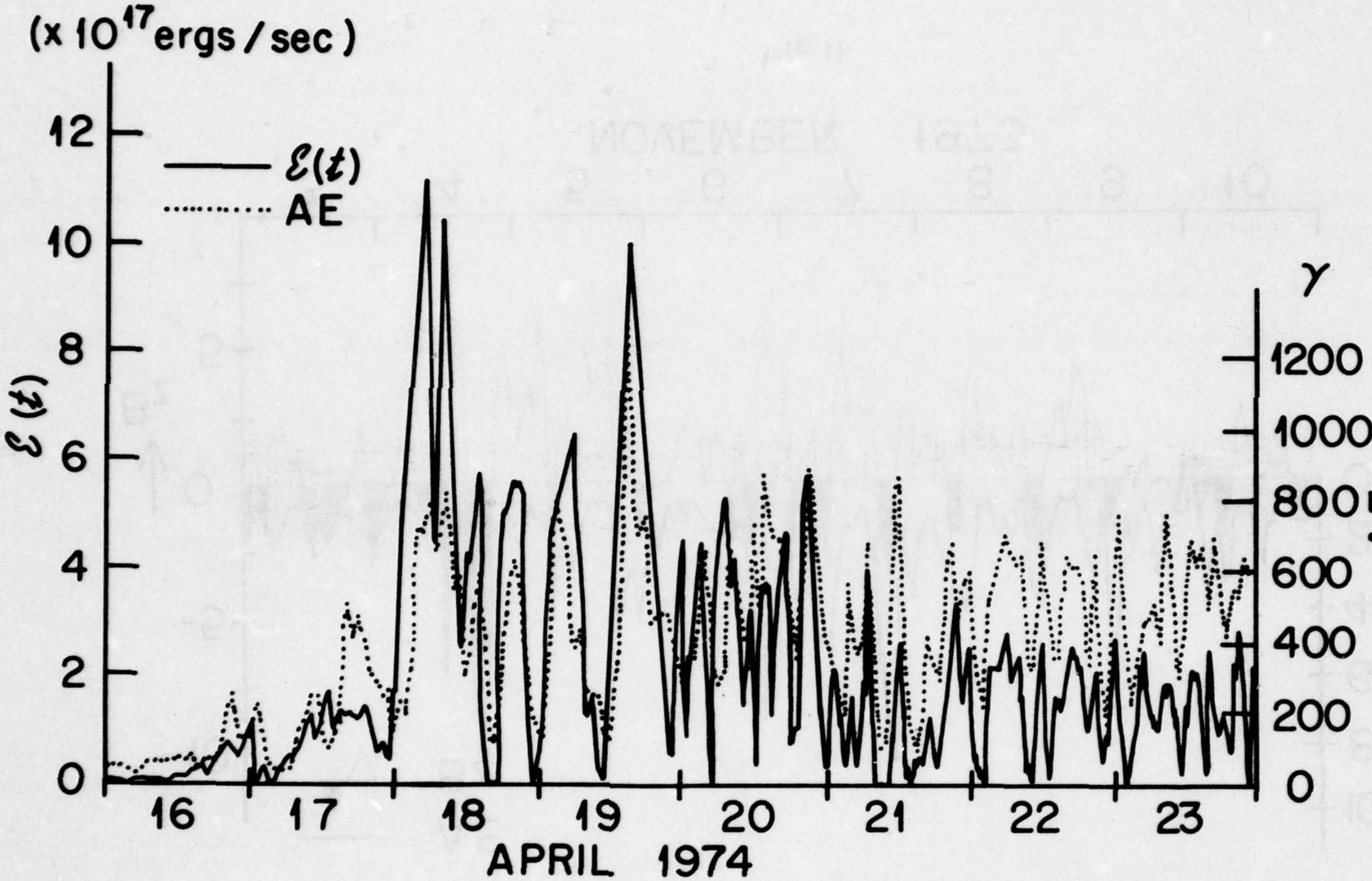
(x 10^17 ergs / sec)
12
10
8
6
4
2
0
ℰ(t)
ℰ(t)
AE
γ
1200
1000
800
600
400
200
0
AE
16
17
18
19
20
21
22
23
APRIL 1974

Fig 2a

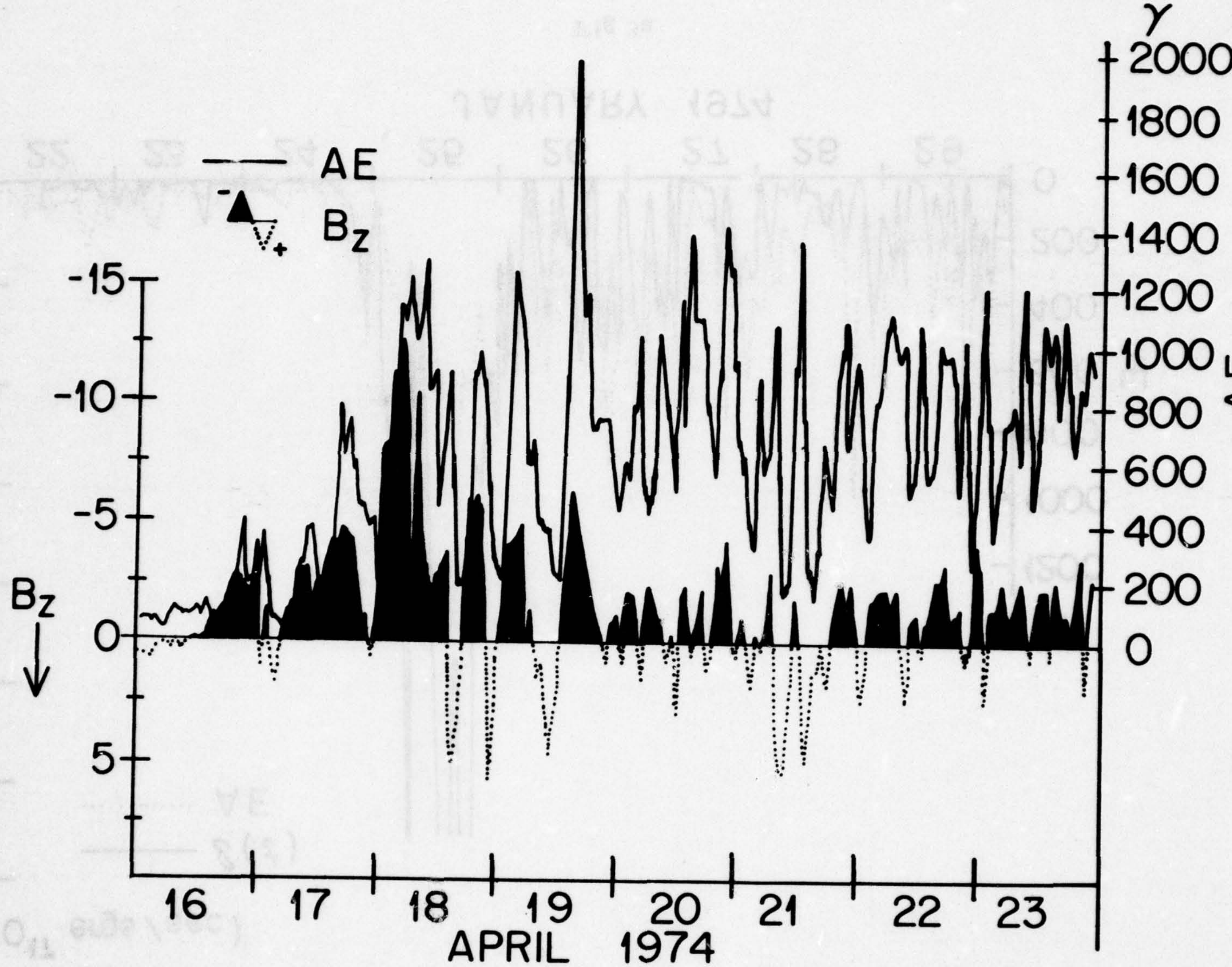

AE
B_z
-15
-10
-5
0
5
B_z
γ
2000
1800
1600
1400
1200
1000
800
600
400
200
0
AE
16
17
18
19
20
21
22
23
APRIL 1974

Fig 2b

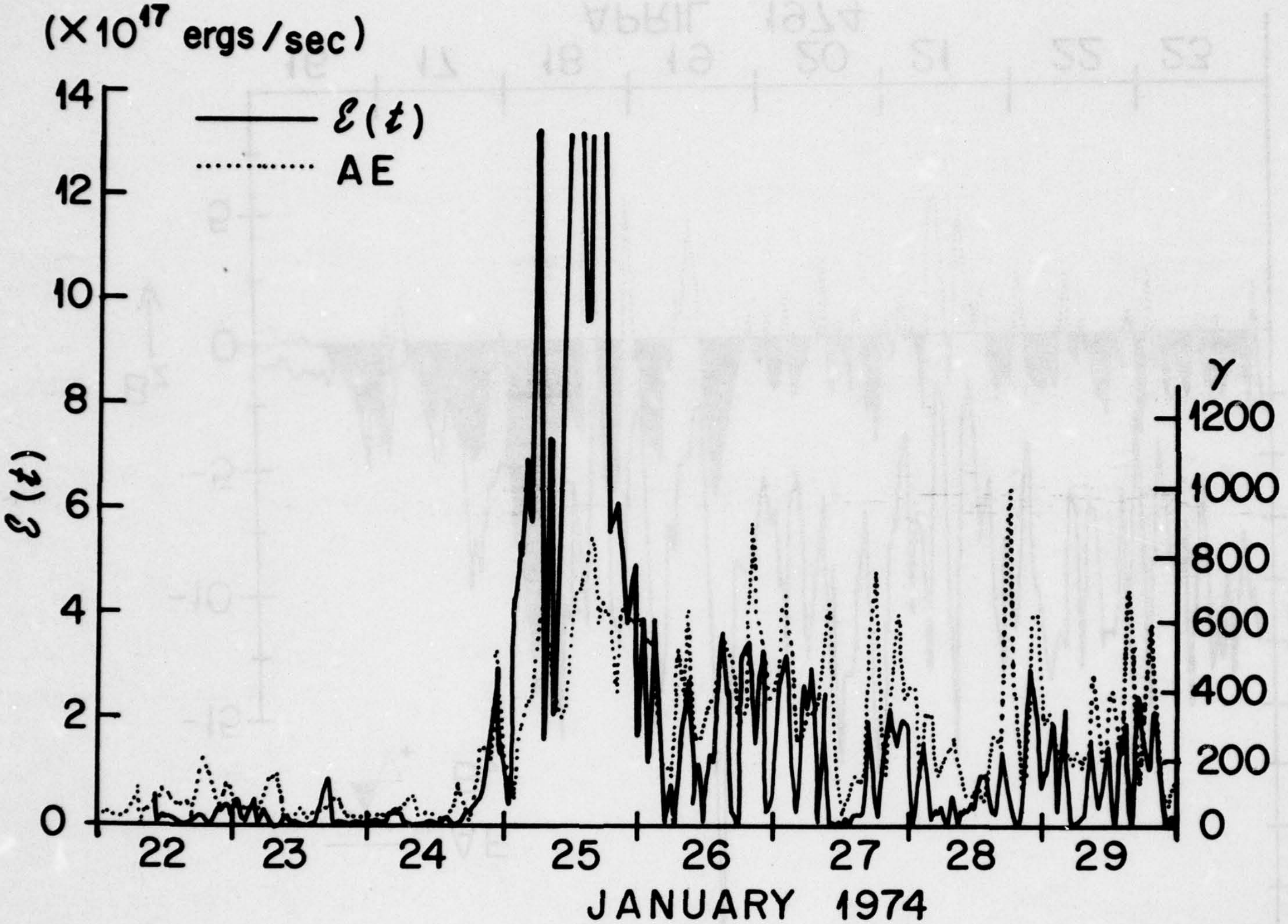
(×10^17 ergs/sec)
ℰ(t)
AE
14
12
10
8
6
4
2
0
22
23
24
25
26
27
28
29
JANUARY 1974
γ
1200
1000
800
600
400
200
0
AE

Fig 3a

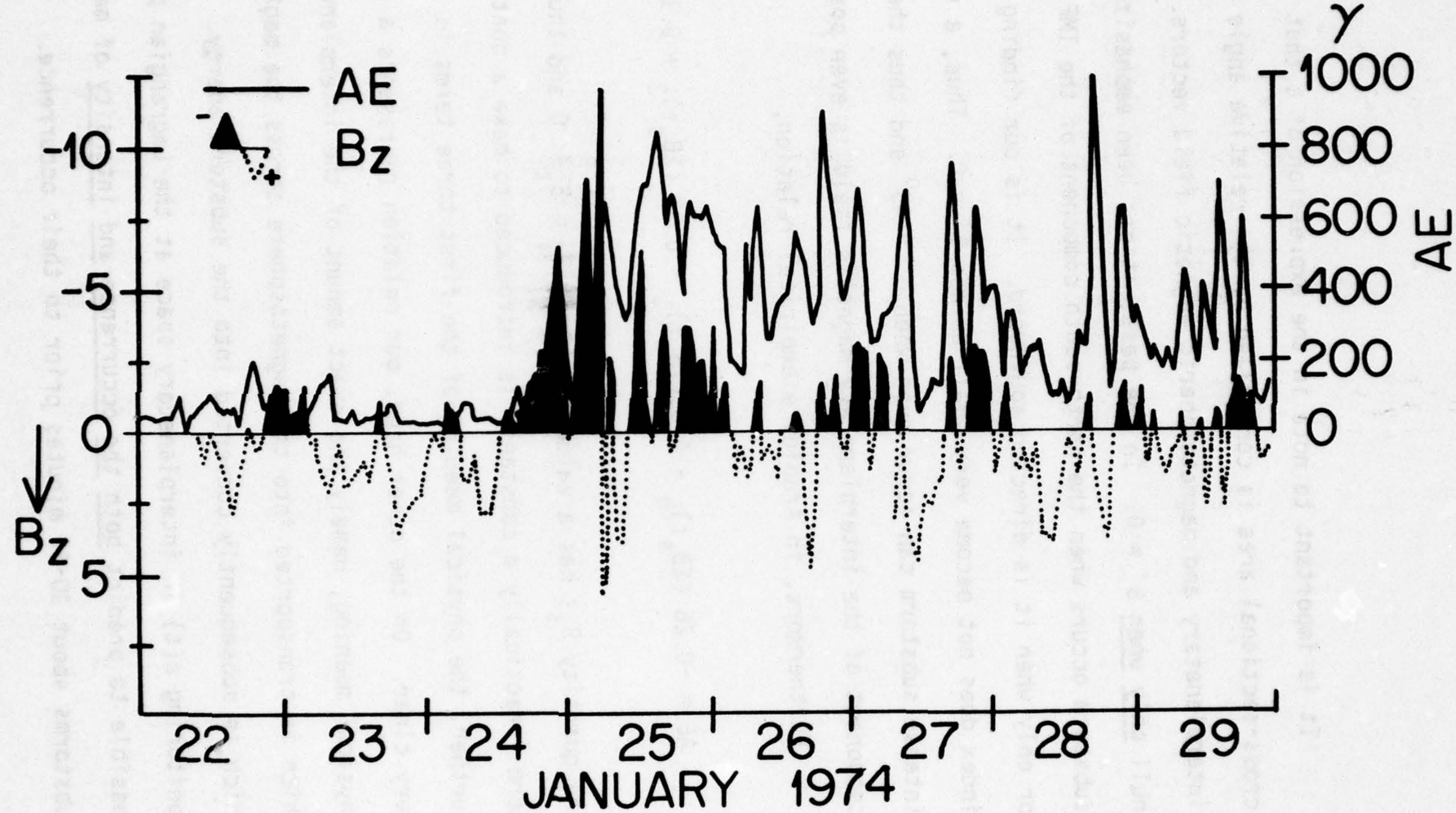

AE
Bz
-10
-5
0
5
Bz
γ
1000
800
600
400
200
0
AE
22
23
24
25
26
27
28
29
JANUARY 1974

Fig 3b

It is important to note in the expression of ε that the size of the cross-sectional area is controlled by the relative angle θ' between the interplanetary and magnetospheric magnetic field vectors. It becomes null only when $\theta' = 0$. In the past, it has been emphasized that a substorm occurs when the north-south component of the IMF becomes negative or only when it is directed southward. It is our finding that the AE index does not become very small unless $\theta' = 0$. Thus, a relatively intense substorm can occur even when $\theta' = 45^{o}$ and thus the north-south component of the interplanetary magnetic field is even positive.

Furthermore, in Arnoldy's empirical relation,

$$AE = -0.26\ (\Sigma B_s\tau)_0 - 0.91(\Sigma B_s\tau)_1 - 0.33\ (\Sigma B_s\tau)_2 + 0.12\ P_0,$$

the quantity $B_s\tau$ has a value only when $B_s = B_z < 0$ and thus the last term (practically a constant) is introduced to make a continuous function. Further, the physical meaning of the first three terms is not necessarily very clear. On the other hand, our relation represents a definite physical meaning, namely the exact amount of the interplanetary energy which is transported into the magnetosphere across the magnetopause which is subsequently converted into the substorm energy. Thus, by monitoring $\varepsilon(t)$ in interplanetary space at the Lagrangian point, it is possible to predict both the occurrence and intensity of magnetospheric substorms about 30-60 minutes prior to their occurrence.

We feel that this finding is a major breakthrough in the search for physically meaningful parameters which can quantitatively predict the occurrence and intensity of substorms.

The quantity $\varepsilon(t)$ is also tested for major geomagnetic storms with a large main phase decrease. It is our finding that the quantity $\varepsilon(t)$ agrees over three orders of magnitude with the total amount of energies produced within the magnetosphere, confirming its accuracy even during violent geomagnetic activity. Figures 4a-c show an example of the comparison between ε and the energy dissipated in the magnetosphere (Perreault and Akasofu, 1978).

(ii) Study of the simultaneous auroral photographs taken from above by the DMSP satellite and from below by the all-sky camera

We made an extensive study of the simultaneous auroral photographs taken from above by the DMSP satellite and from below by the all-sky camera at the South Pole Station. Figures 5a through 5g show a complete set of data for June 12, 1975. Each figure shows a DMSP photograph and the simultaneous all-sky photograph taken from the South Pole. The location of the South Pole in the DMSP photograph is indicated by a white dot; the location of the invariant pole is indicated by a white cross; the noon meridian by a white line. In the all-sky photograph, the direction of the invariant pole is indicated by a white bar near the edge of the circular photograph. Each figure shows several all-sky photographs taken shortly before and after the satellite passage. Both DMSP and all-sky photographs complement each other (the former provide a large-scale view, and the latter provide fine-time-scale data). For more details, see Akasofu (1978).

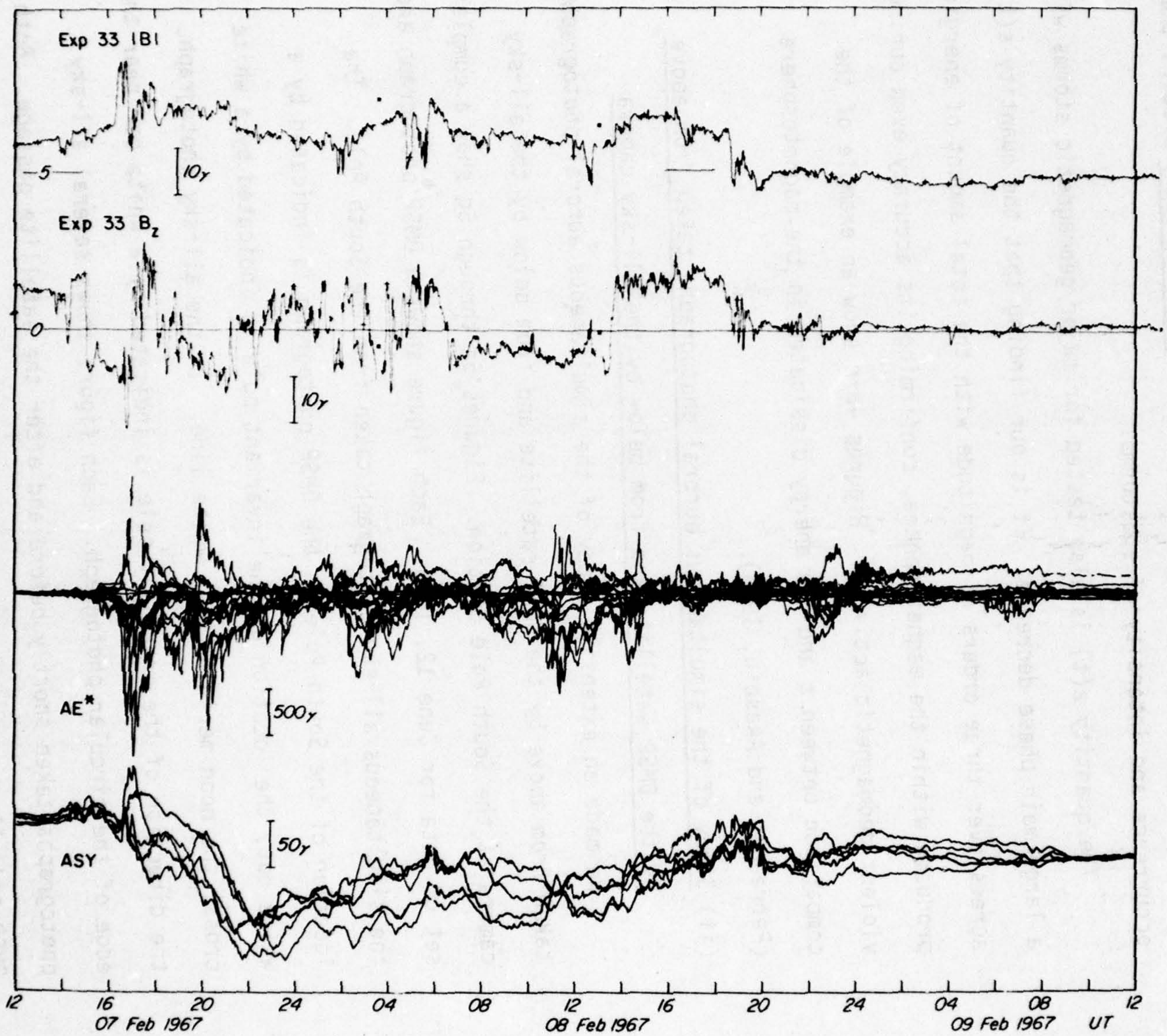

Exp 33 |B|
5
10γ
Exp 33 B_z
0
10γ
AE*
500γ
ASY
50γ
12 16 20 24 04 08 12 16 20 24 04 08 12
07 Feb 1967
08 Feb 1967
09 Feb 1967
UT

Fig 4a

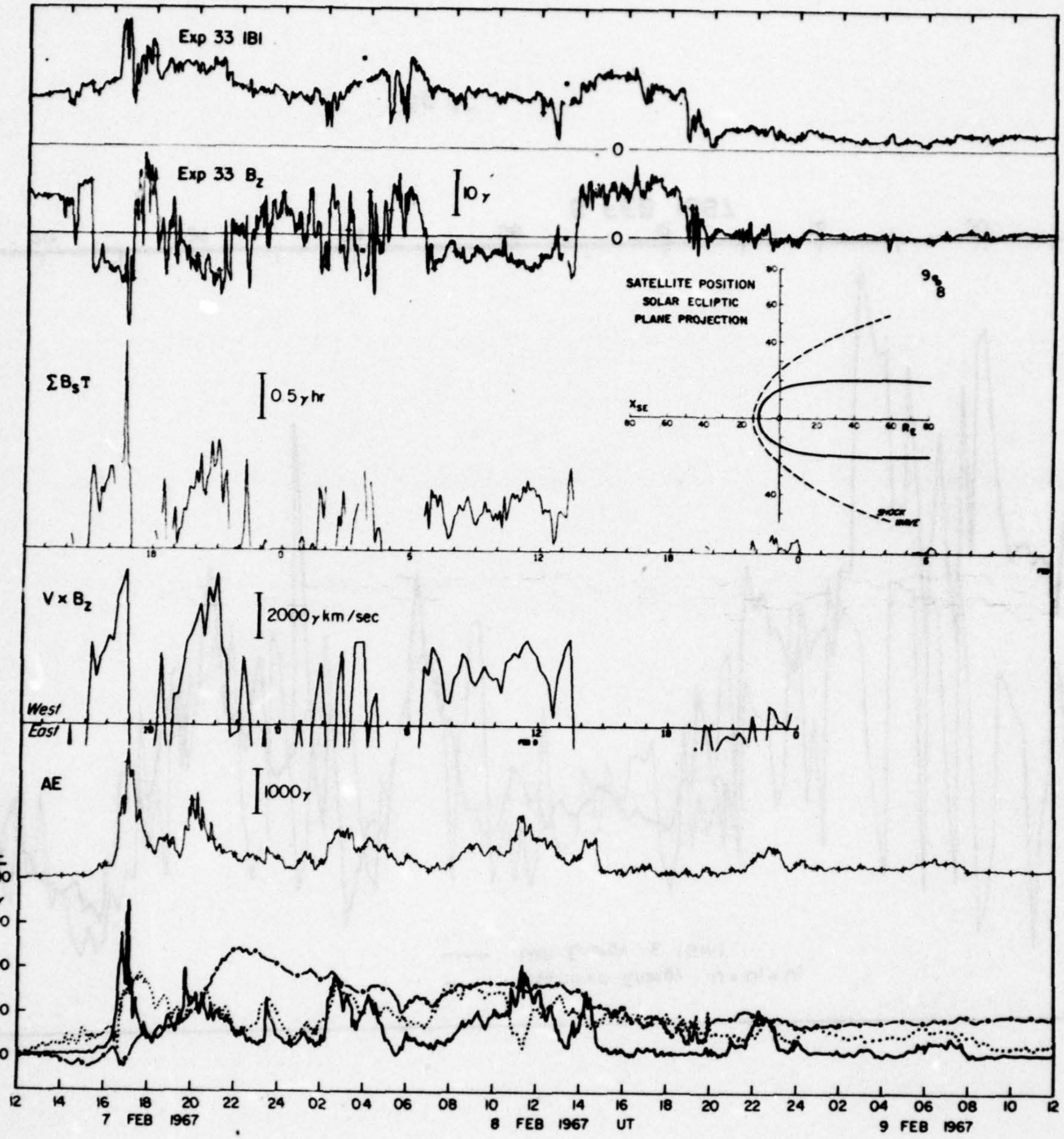

Exp 33 |B|
Exp 33 B_z
10 γ
0
SATELLITE POSITION
SOLAR ECLIPTIC
PLANE PROJECTION
X_{SE}
R_E
SHOCK WAVE
$\Sigma B_S T$
0.5 γ hr
V x B_z
2000 γ km/sec
West
East
AE
1000 γ
DST(-)
ASY
AL
200 γ 150 100 50 0
2000 γ 1500 1000 500 0
12 14 16 18 20 22 24 02 04 06 08 10 12 14 16 18 20 22 24 02 04 06 08 10 12
7 FEB 1967
8 FEB 1967 UT
9 FEB 1967

Fig 4b

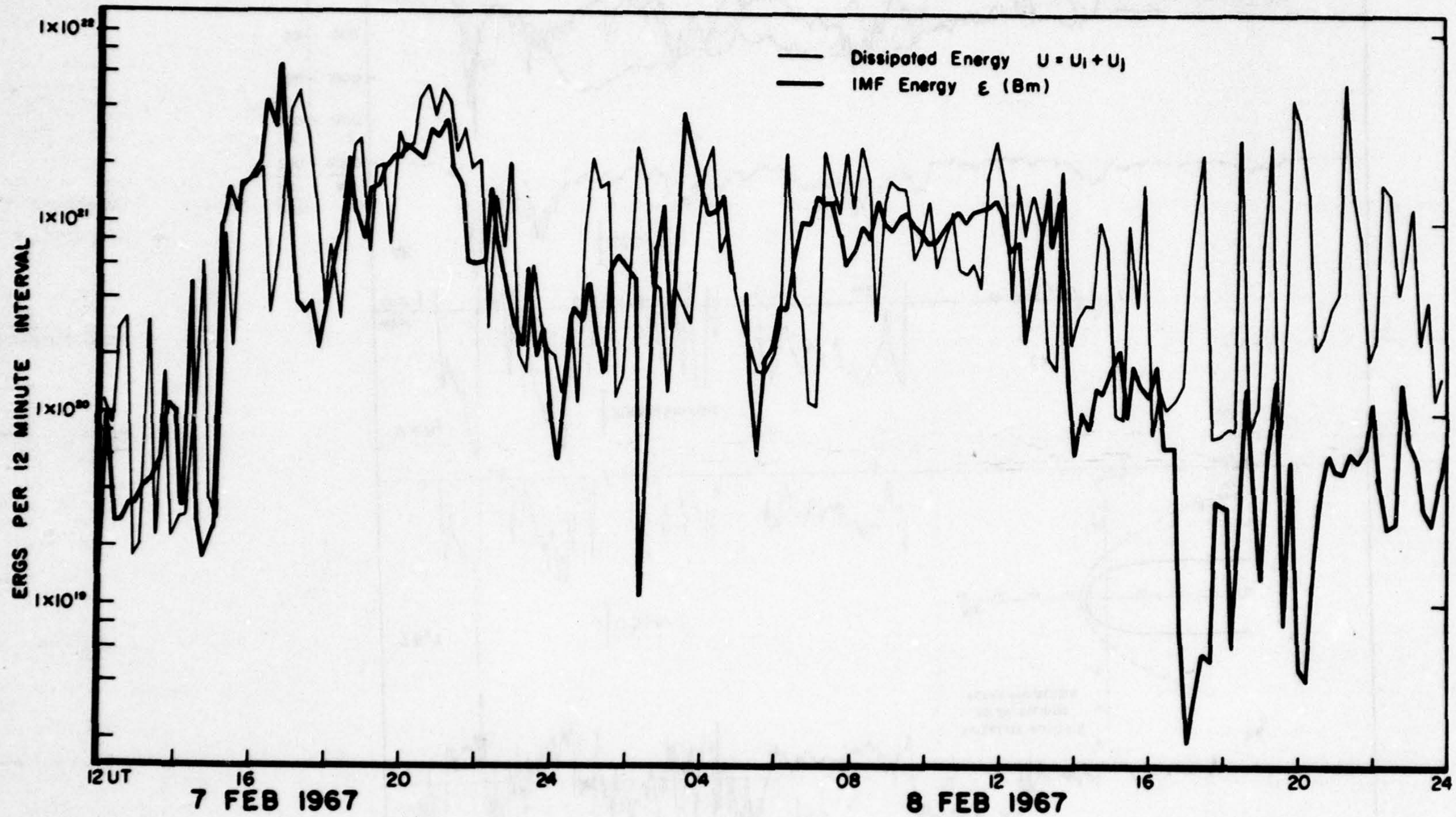
Dissipated Energy U = U_I + U_J
IMF Energy ε (Bm)
ERGS PER 12 MINUTE INTERVAL
1x10^22
1x10^21
1x10^20
1x10^19
12 UT
16
20
24
04
08
12
16
20
24
7 FEB 1967
8 FEB 1967

Fig 4c

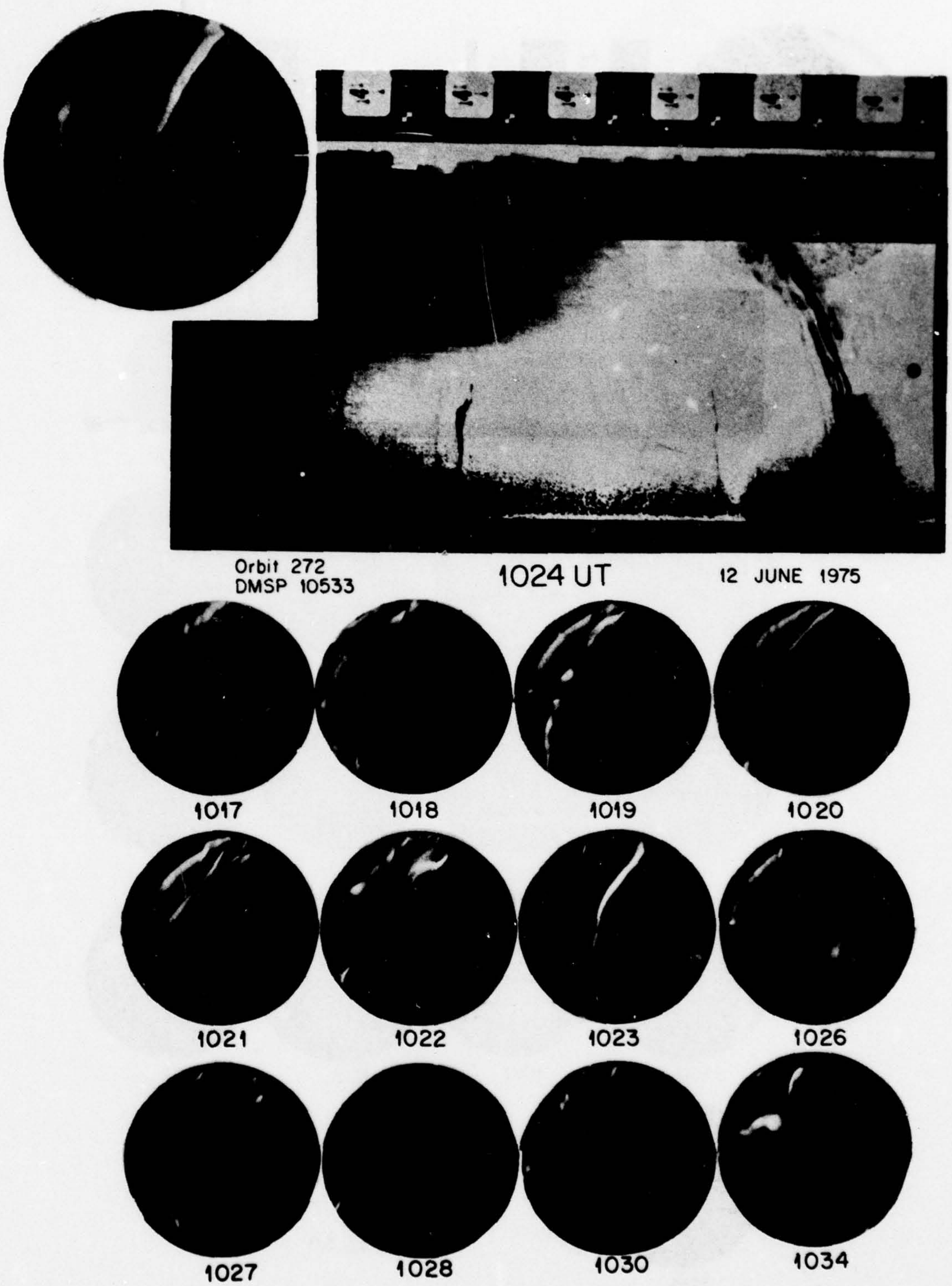
Orbit 272
DMSP 10533
1024 UT
12 JUNE 1975
1017
1018
1019
1020
1021
1022
1023
1026
1027
1028
1030
1034

Fig 5a

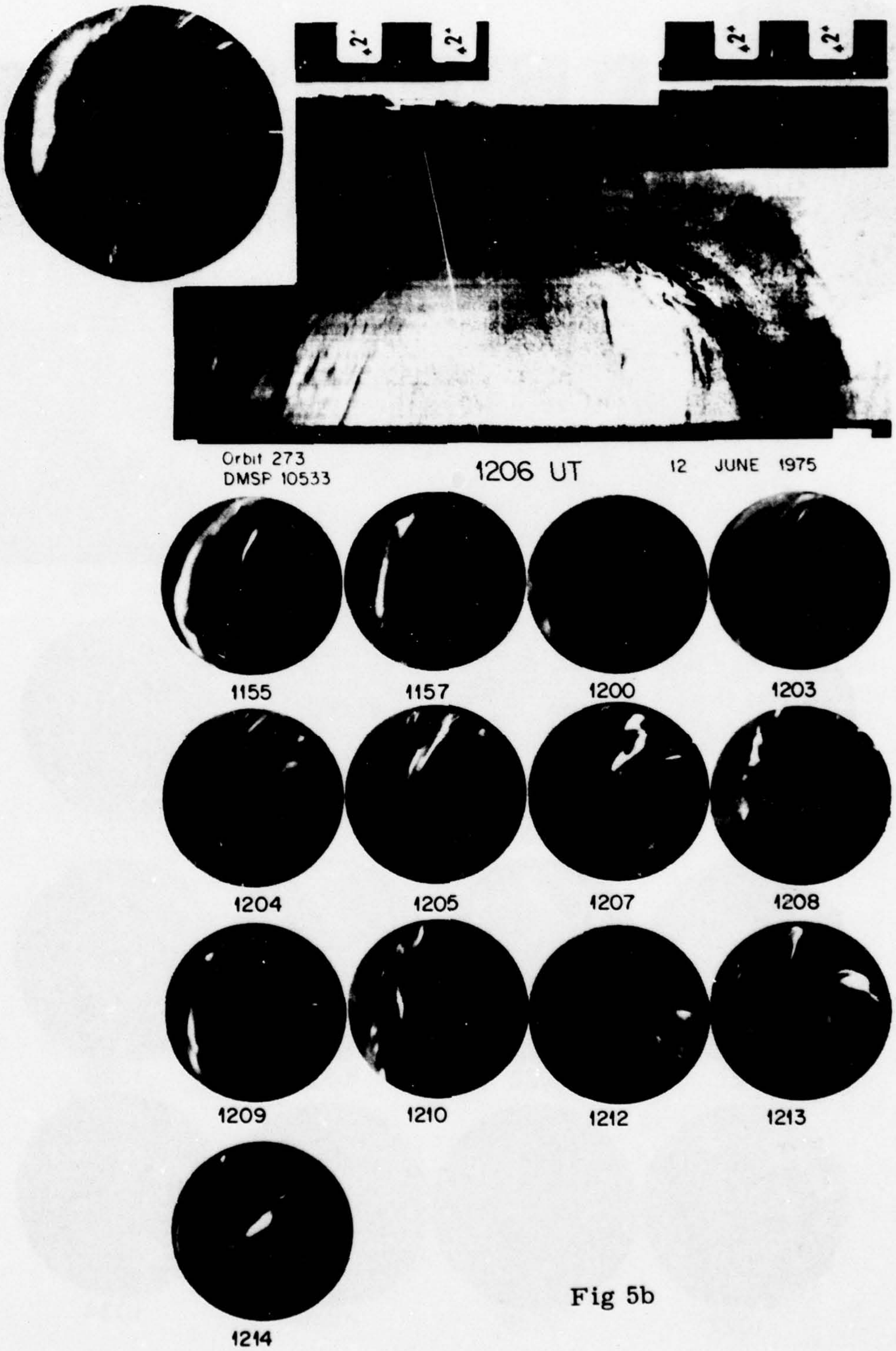
2°
2°
2°
2°
Orbit 273
DMSP 10533
1206 UT
12 JUNE 1975
1155
1157
1200
1203
1204
1205
1207
1208
1209
1210
1212
1213
1214

Fig 5b

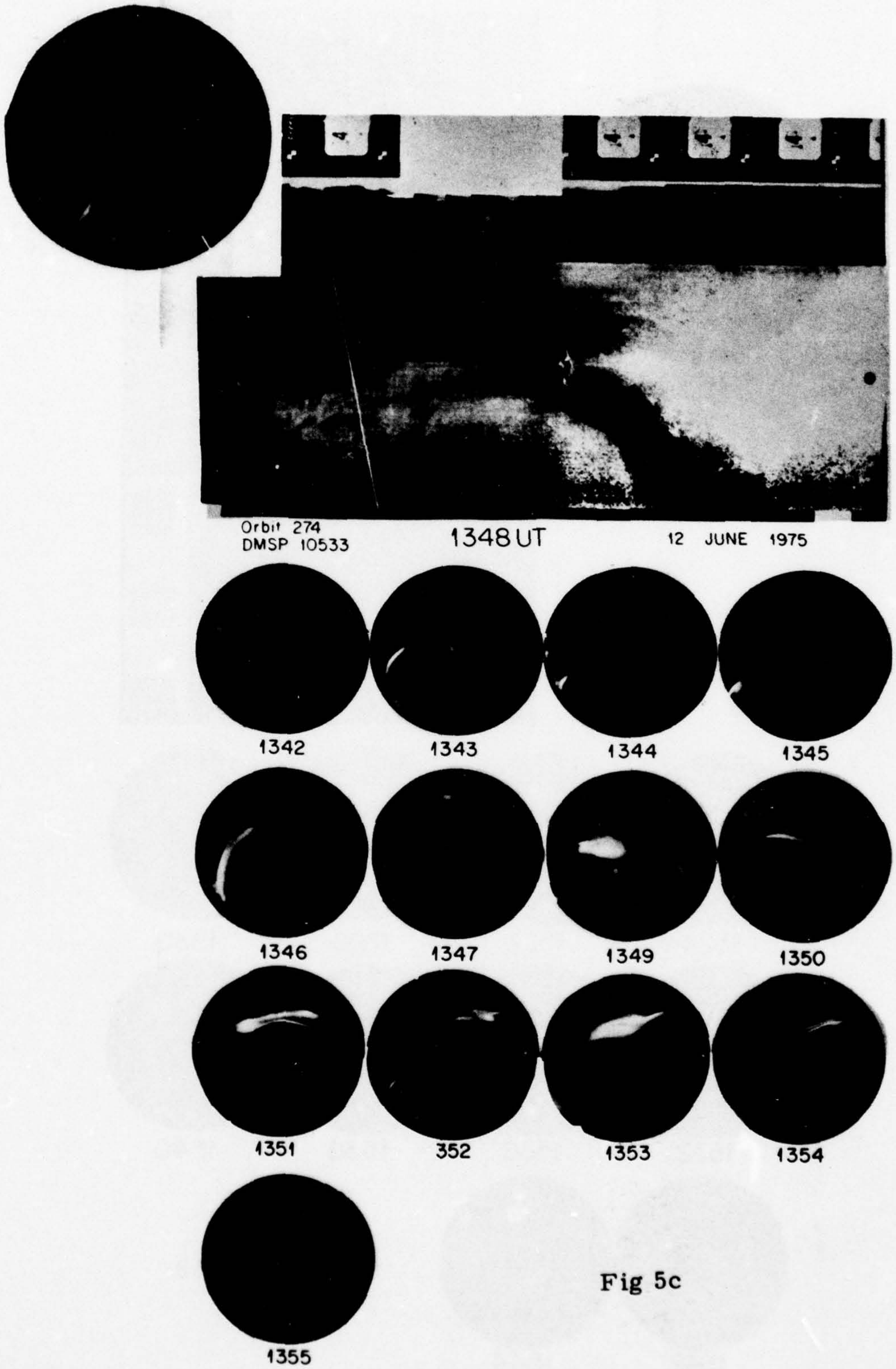
Orbit 274
DMSP 10533
1348 UT
12 JUNE 1975
1342
1343
1344
1345
1346
1347
1349
1350
1351
352
1353
1354
1355

Fig 5c

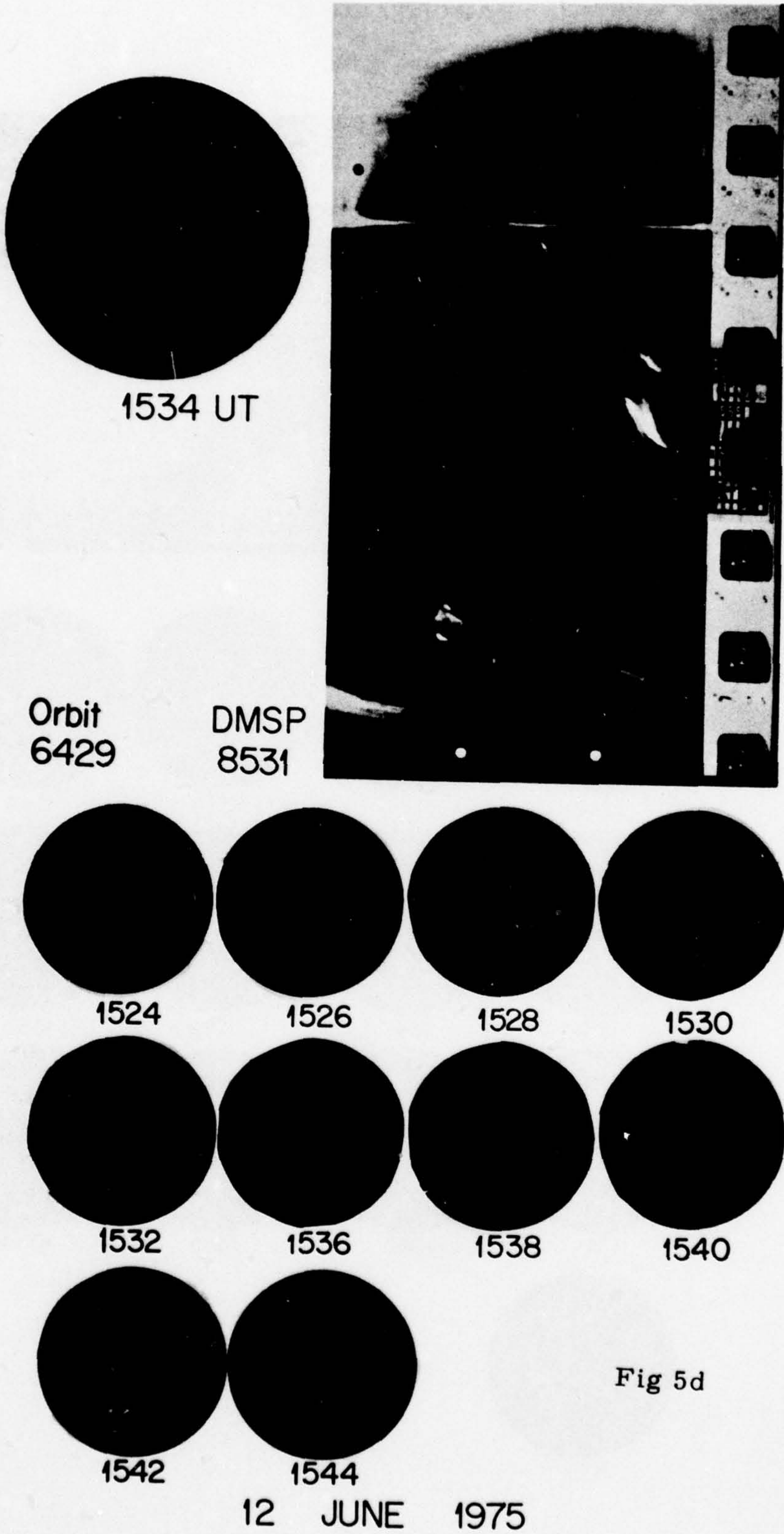
1534 UT
Orbit
6429
DMSP
8531
1524
1526
1528
1530
1532
1536
1538
1540
1542
1544
12 JUNE 1975

Fig 5d

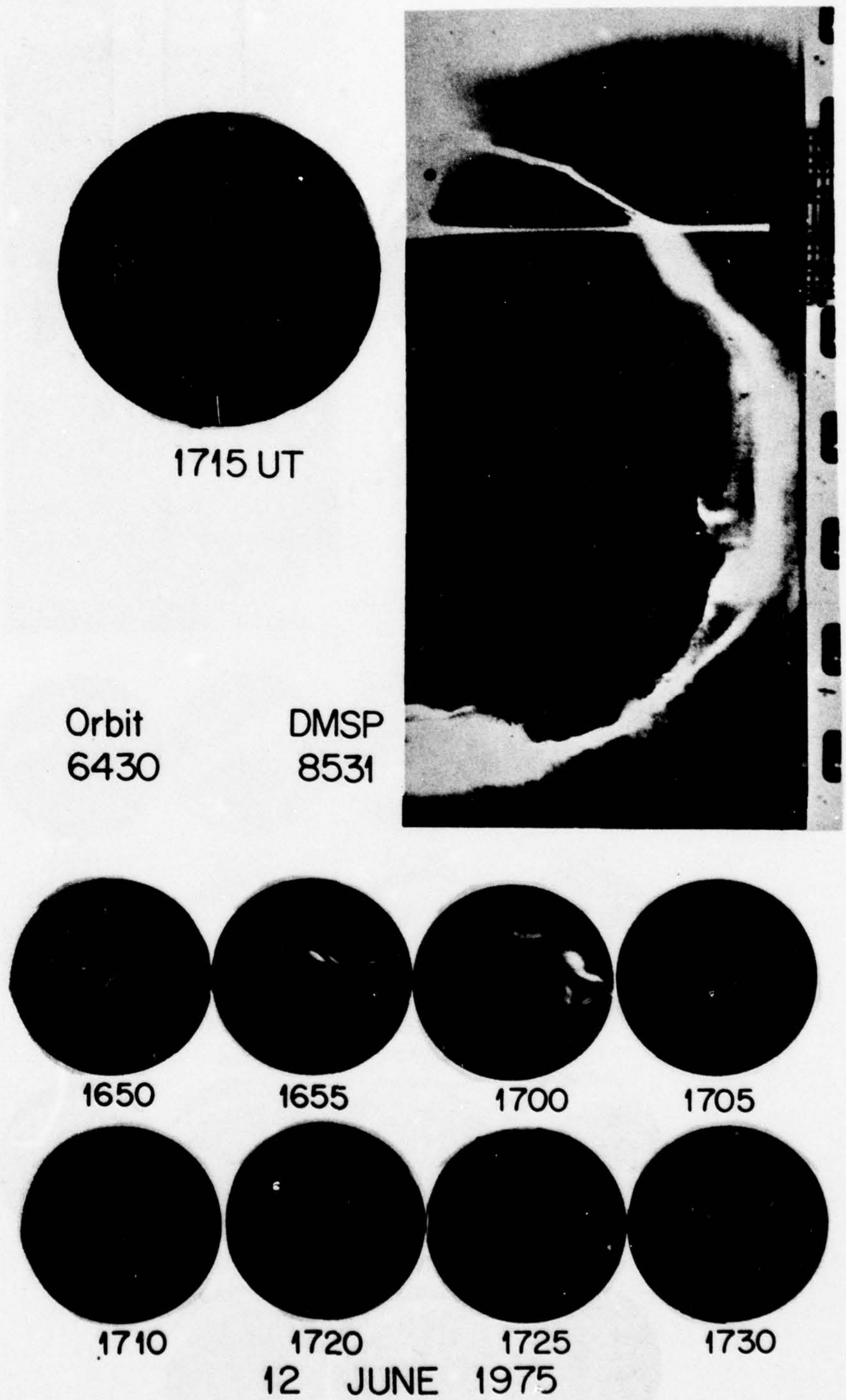
1715 UT
Orbit
6430
DMSP
8531
1650
1655
1700
1705
1710
1720
1725
1730
12 JUNE 1975

Fig 5e

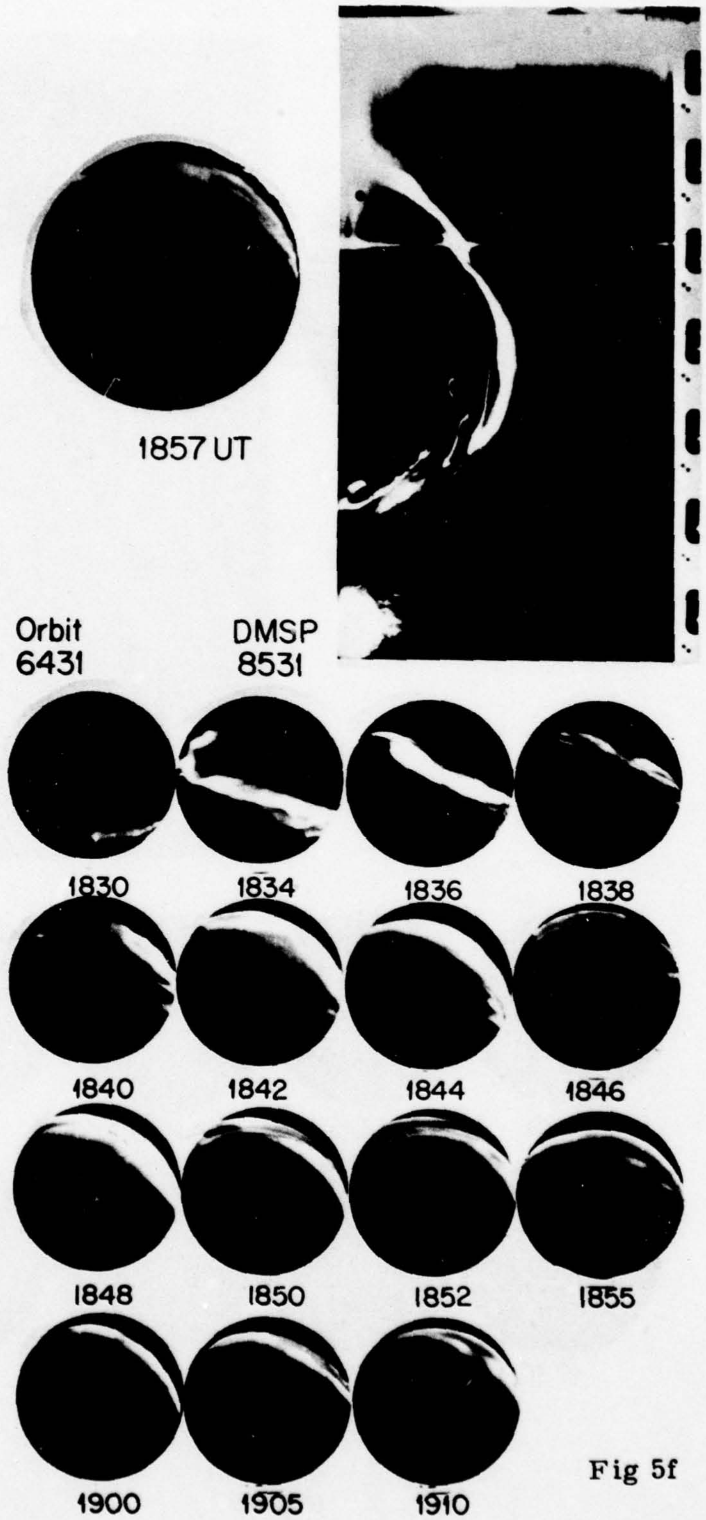

Fig 5f

12 JUNE 1975

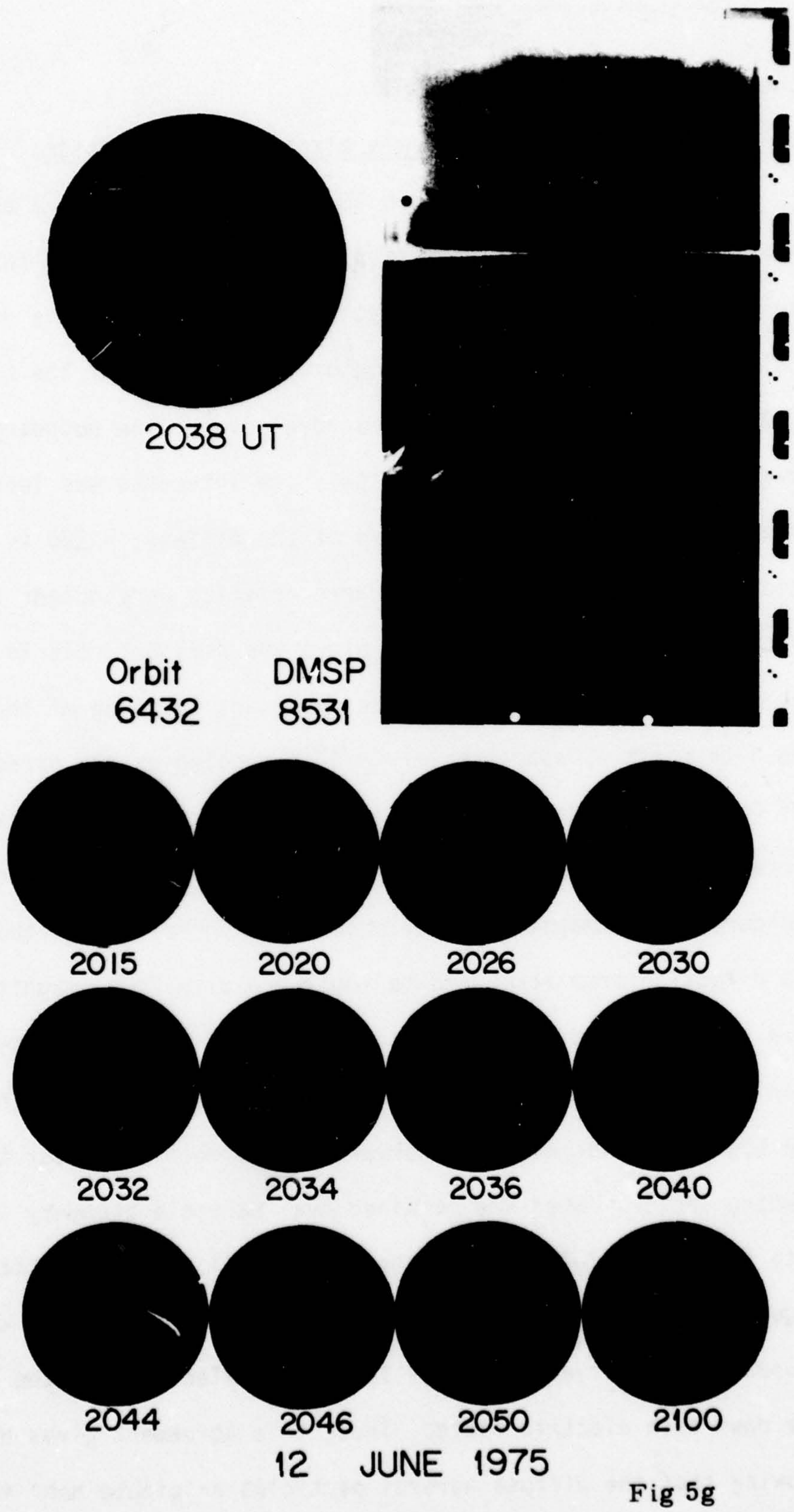
2038 UT
Orbit
6432
DMSP
8531
2015
2020
2026
2030
2032
2034
2036
2040
2044
2046
2050
2100
12 JUNE 1975

Fig 5g

Other Results

(i) Equatorward boundary of the electron precipitation

Electron spectrograms from 351 passes of the Isis 1 and 2 satellites were utilized to study statistically the effects of the interplanetary magnetic field (IMF), substorm activity, and the earth's dipole tilt angle on the latitude of the equatorward boundary of the nightside (2000-0400 magnetic local time) auroral oval. The boundary location (in invariant latitude) at hourly local time intervals was identified in terms of the equatorward boundary of the diffuse, > 100 eV electron precipitation. The following characteristics were noted: (1) The north-south component (B_z) of the IMF plays the dominant role in controlling the motion of this boundary. The invariant latitude of the boundary is shown to shift by approximately $\pm 4^o$ depending on the direction of the IMF (northward and southward, respectively) relative to its position corresponding to $B_z = 0$. This indicates an inward motion of the associated boundary in the magnetotail by about 5 earth radii when the IMF changes its direction from northward to southward with large magnitude. There is a significant difference in the amount of the shift between the evening and morning sectors, i.e., for the same decrease in B_z value, the boundary moves more equatorward in the morning sector than in the evening sector. When the obtained oval particle boundary is projected onto the equatorial plane of the magnetotail along magnetic field lines, a good agreement was found between the projected boundary and the drift boundary (the Alfvén layer) of low energy electrons in the presence of the dawn-dusk electric field. Thus, this agreement gives new evidence showing that the diffuse auroral particles originate near and at the

inner boundary of the plasma sheet. (2) Substorm activity seems to have a separate role in determining the latitude of the equatorward boundary of the nightside auroral precipitation region. The boundary during substorm periods is statistically found to be 2 - 3^{o} lower in invariant latitude than that during quiet times. Even a simple classification into quiet and disturbed conditions improves the accuracy with which the auroral oval location can be inferred. By combining the IMF effect and the substorm effect, it is indicated that the boundary is located at the lowest latitudes when a substorm takes place during a southward IMF with large magnitude, whereas it is located in the highest latitudes when the IMF has a northward component during quiet times. (3) The equatorward boundary of the nightside auroral oval is located in higher latitudes in the winter hemisphere than in the summer hemisphere, although this earth's dipole tilt effect is usually smaller than the effects of the IMF and substorm activity. For more details, see Kamide et al. (1978).

(ii) Correlation study between the power of the meter-wave radiation and the AE index

In the past several years low frequency radio measurements have shown that the earth's magnetosphere is a very intense radio emitter, with characteristics very similar to other astronomical radio sources such as Jupiter and Saturn. Gurnett showed that these radio emissions are closely associated with the occurrence of auroral arcs on the night side of the earth. Both the angular distribution of the emitted radiation and direction finding measurements indicate that such an intense (up to 10^9 watts, total radiated power) radiation associated with auroral arcs is generated at relatively low altitudes ($\sim 3\ R_E$ radial distance) over

the night and evening auroral regions, presumably by the intense fluxes of several keV electrons, causing the aurora and the currents responsible for the magnetic disturbances. Because of the close association with auroral phenomena and the wavelengths in the kilometer range these radio emissions have been called auroral kilometric radiation.

Although kilometric radiation is known to be associated with high latitude magnetic disturbances little has been done to study this relationship in detail. It is of interest to determine just how good the correlation is and whether there are any exceptions to the observed relationship. The relationship of the radio emission intensity to the currents flowing through the auroral zone may, for example, be helpful in developing a better understanding of how the auroral kilometric radiation is generated. Furthermore, since radio emissions from the entire auroral zone can be easily monitored by a single spacecraft there is the question of whether the auroral kilometric radiation intensity could provide, on a near real time basis, a parameter which is comparable to magnetic disturbance indices, such as the auroral electrojet index, AE, which require a large array of ground stations with the attendant problems of information retrieval and processing. We made a detail study of the relationship between the auroral kilometric radiation intensities observed by the IMP-6 spacecraft and the AE index computed from a series of high-latitude magnetometer station and demonstrated that the auroral kilometric radiation is a good indicator of auroral magnetic disturbances (Figures 6a and 6b); for more details, see Voots et al. (1977).

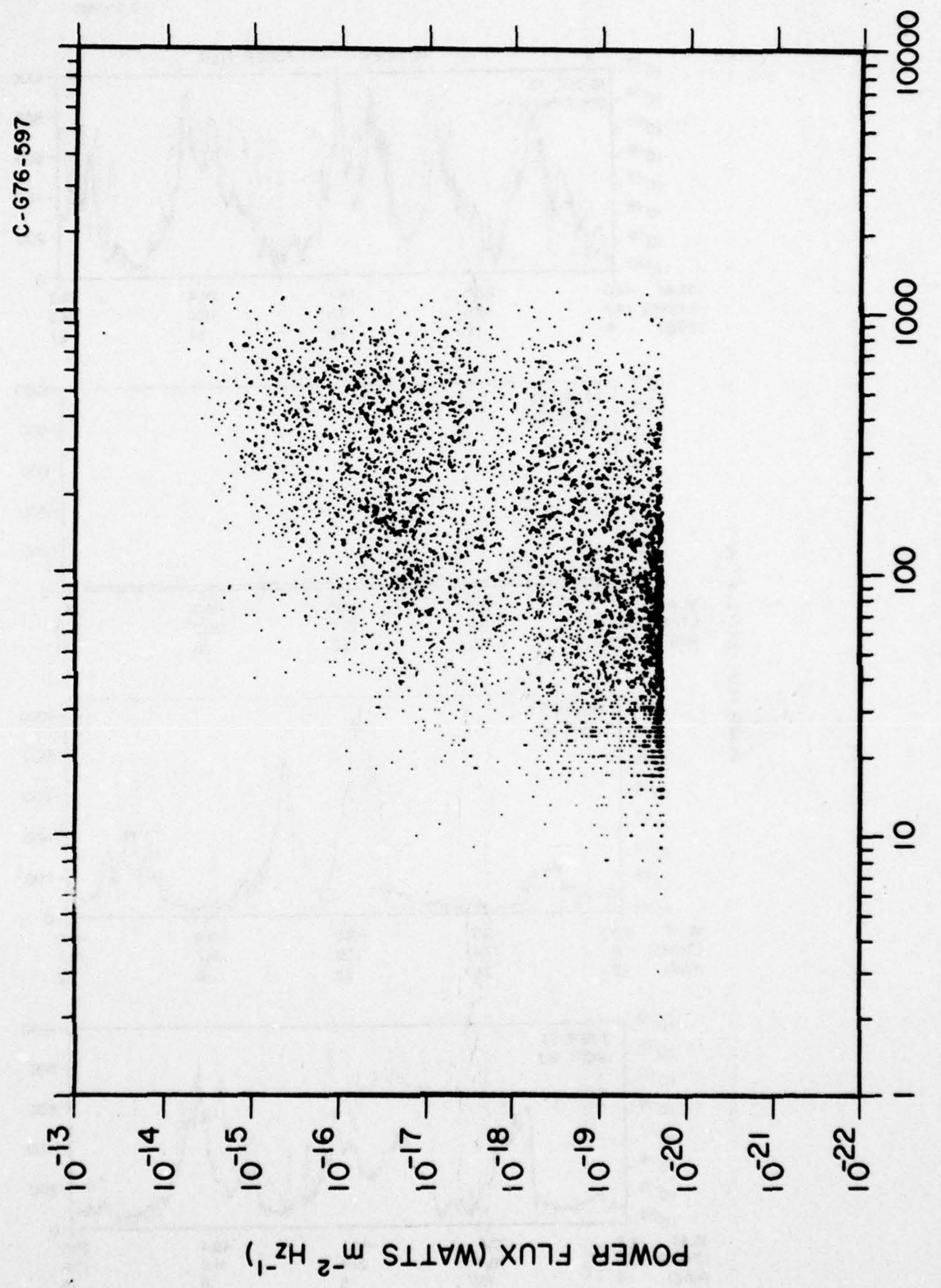

C-G76-597
POWER FLUX (WATTS m^{-2} Hz^{-1})
10^{-13}
10^{-14}
10^{-15}
10^{-16}
10^{-17}
10^{-18}
10^{-19}
10^{-20}
10^{-21}
10^{-22}
1
10
100
1000
10000
AE INDEX (γ)

Fig 6a

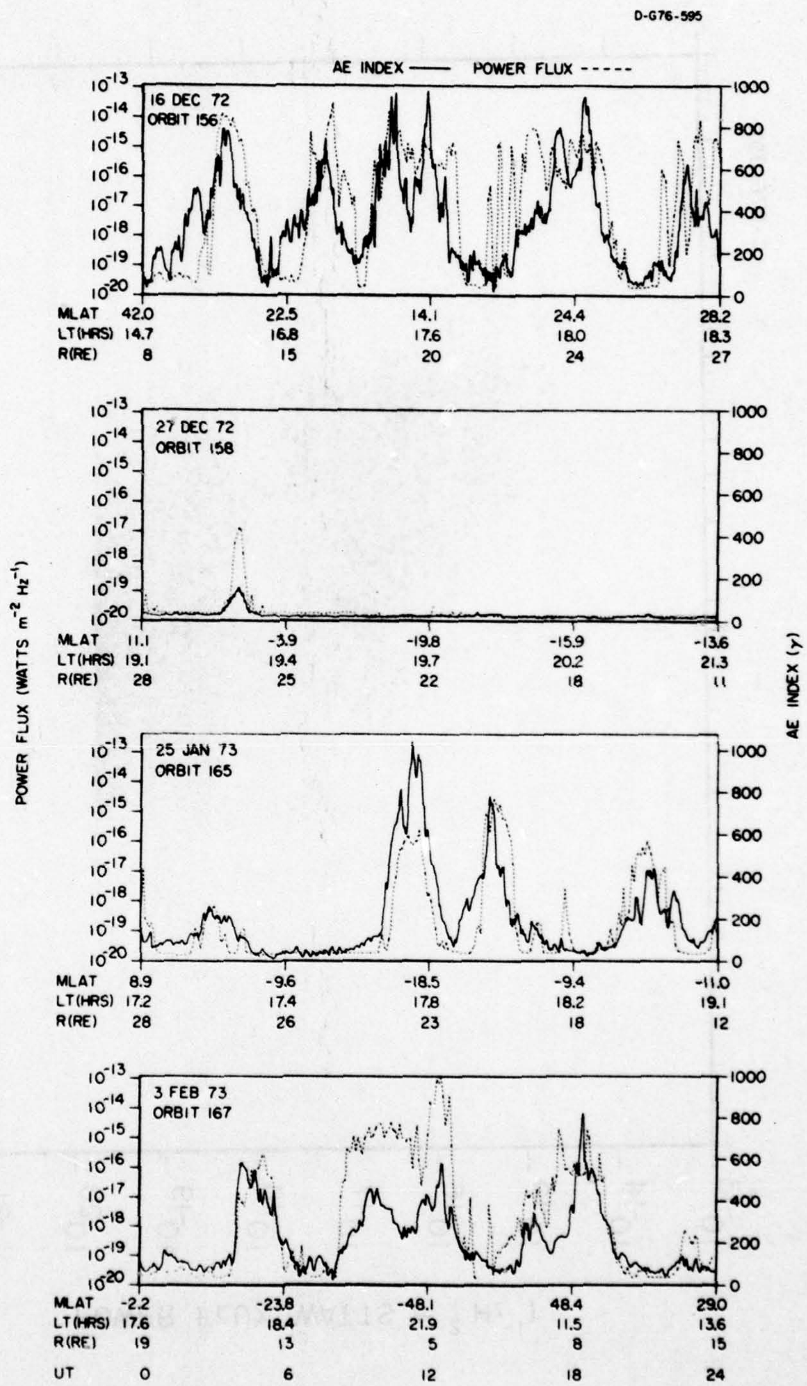
D-G76-595
AE INDEX ——— POWER FLUX - - - - -
16 DEC 72
ORBIT 156
27 DEC 72
ORBIT 158
25 JAN 73
ORBIT 165
3 FEB 73
ORBIT 167
POWER FLUX (WATTS m^{-2} Hz^{-1})
AE INDEX (γ)
MLAT 42.0 22.5 14.1 24.4 28.2
LT(HRS) 14.7 16.8 17.6 18.0 18.3
R(RE) 8 15 20 24 27
MLAT 11.1 -3.9 -19.8 -15.9 -13.6
LT(HRS) 19.1 19.4 19.7 20.2 21.3
R(RE) 28 25 22 18 11
MLAT 8.9 -9.6 -18.5 -9.4 -11.0
LT(HRS) 17.2 17.4 17.8 18.2 19.1
R(RE) 28 26 23 18 12
MLAT -2.2 -23.8 -48.1 48.4 29.0
LT(HRS) 17.6 18.4 21.9 11.5 13.6
R(RE) 19 13 5 8 15
UT 0 6 12 18 24

Fig 6b

(iii) Auroral circle

The accurate determination of the shape of the auroral oval is an important problem in magnetospheric physics, as well as in predicting the location of the oval. C.-I. Meng, R.H. Holzworth and the Principal Investigator made an extensive study on this subject by analyzing more than fifty DMSP auroral photographs. It is found that the poleward boundary of the auroral oval can be fitted by an off-centered circle within an accuracy of less than 0.5^{o} in latitude; for more details, see Meng et al. (1977).

(iv) Polar cap arcs

It has been well established that auroras tend to appear along an oval band known as the auroral oval. However, there is another type of aurora which appears well inside the area bounded by the auroral oval, namely polar cap auroras. C.-I. Meng and the Principal Investigator have found several DMSP auroral photographs which show polar cap arcs which lie parallel to oval arcs by changing the orientation, from the sun-earth line (or the noon-midnight meridian) direction to the westward direction, near the poleward boundary of the oval in the night sector; for more details, see Meng and Akasofu (1976).

(v) Response of the dayside aurora to sharp northward and southward transitions of the interplanetary magnetic field and to magnetospheric substorms

Latitudinal shifts of the dayside aurora are examined with respect to variations in the interplanetary magnetic field (IMF) and to magnetospheric substorms. Within 10-15 minutes after steplike southward (northward) transitions in the IMF, the dayside auroral oval moves equatorward

(poleward). In some cases, the auroral shift is similar to an exponential relaxation in latitude from an initial to a final steady state value; for these cases, the average exponential time constant is estimated to be 17 minutes. Substorm features in the dayside aurora include: (a) an equatorward shift by 1^o to 3^o at the equatorward auroral boundary, (b) a brightening of the aurora near substorm onset, (c) the formation of multiple auroral bands and (d) poleward motion of individual auroral arcs occurring nearly coincident in time with the equatorward boundary shifts, the average poleward velocity of these arcs being approximately 800 m/sec.

(vi) HF radio wave absorption

It has been well known that auroral activity causes a heavy absorption of HF radio waves. However, because of a lack of an appropriate array of riometer stations, the latitudinal development of cosmic noise absorption during auroral substorms has not been accurately known.

The operation of both all-sky camera and riometers along the Alaskan meridian in 1973 made such a study possible. Changes of the latitudinal distribution of auroras were carefully examined over a latitudinal range of more than 10^0, and the simultaneous changes were obtained by using a computer contouring technique. A paper on this subject is now near completion (Berkey, Anger and Akasofu).

(vii) Auroral motions and the (ExB) drift motion of ionospheric plasma

It has been an important question whether or not auroral motions represent the (ExB) convective motion. Past studies suggested that the poleward motion of auroras during the expansive phase is not the (ExB) motion, but the eastward motions in morning hours are. However, there

had been no extensive study of this important subject, since a systematic monitoring of the ionospheric electric field was not available until 1970, when the Chatanika incoherent scatter radar came into existence.

However, during the last several years, a large amount of high quality electric field measurements and the simultaneous all-sky photographs became available. Therefore, we made an extensive study of the correlation between the two data sets. The results are shown in Figure 7. Our main result is that auroral motions are generally far from the (ExB) drift motion in the ionospheric level. Often, they are opposite to the (ExB) drift motion.

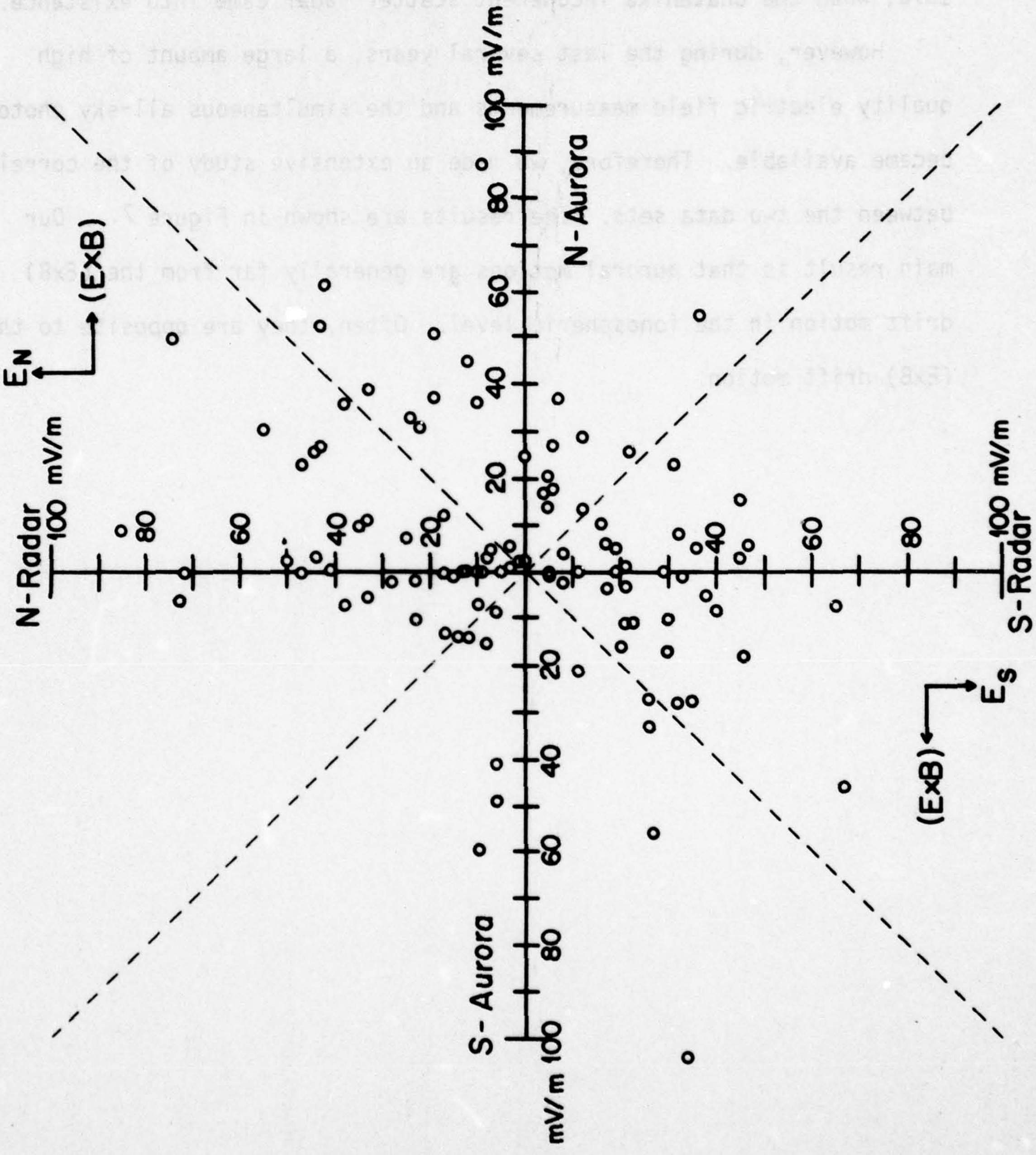
N-Radar
S-Radar
N-Aurora
S-Aurora
100 mV/m
80
60
40
20
20
40
60
80
100 mV/m
100 mV/m
80
60
40
20
20
40
60
80
mV/m 100
(E×B)
E_N
(E×B)
E_S

Fig 7

References

Akasofu, S.-I., Recent progress in antarctic auroral studies, Upper Atmosphere Research in Antarctica, Antarctic Research Series, 29, American Geophysical Union, 1978.

Arnoldy, R.L., Signature in the interplanetary meridian for substorms, J. Geophys. Res., 76, 5189, 1971.

Ballif, J.R., D.E. Jones and P.J. Coleman, Jr., Further evidence on the correlation between transverse fluctuation in the interplanetary magnetic field and Kp, J. Geophys. Res., 74, 2289, 1969.

Kamide, Y., P.D. Perreault, S.-I. Akasofu and J.D. Winningham, Dependence of substorm occurrence probability on the interplanetary magnetic field and on the size of the auroral oval, J. Geophys. Res., 82 5521, 1978.

Meng, C.-I. and S.-I. Akasofu, The relationship between the polar cap auroral arc and the auroral oval arc, J. Geophys. Res., 81, 4001, 1976.

Meng, C.-I., R.H. Holzworth and S.-I. Akasofu, Auroral circle, delineating the poleward boundary of the quiet auroral belt, J. Geophys. Res., 82, 164, 1977.

Olbert, S., Summary of experimental results from M.I.T. dectector on IMP-1, Physics of the Magnetosphere (ed. by R.L. Carovillano, J.F. McClay and H.R. Radoski), P. 641, D. Reidel Pub. Co, Dordrecht-Holland, 1968.

Perreault, P. and S.-I. Akasofu, A study of geomagnetic storms, Geophys. J. Roy. Astron. Soc., 54, (in press), 1978.

Snyder, C.W., M. Neugebauer and U.R. Rao, The solar wind velocity and its correlation with cosmic-ray variations and with solar and geomagnetic activity, J. Geophys. Res., 68, 6361, 1963.

Voots, G.R., D.A. Gurnett and S.-I. Akasofu, Auroral kilometric radiation as an indicator of auroral magnetic disturbances, J. Geophys. Res., 82, 2259, 1977.

Figure Captions

Figure 1a Correlation between the auroral electrojet index AE and the interplanetary quantity $\varepsilon(t)$ for the November 3-10, 1973 storm.

Figure 1b Correlation between the auroral electrojet index AE and the B_z component of the interplanetary magnetic field (IMF) for the November 3-10, 1973 storm. The B_z component is plotted in reverse and negative periods are hatched; positive periods are plotted by a dotted line.

Figure 2a Correlation between the AE index and $\varepsilon(t)$ for the April 16-23 storm.

Figure 2b Correlation between the AE index and the B_z component of the IMF for the April 16-23, 1974 storm; for details, see the caption for Figure 1a.

Figure 3a Correlation between the AE index and $\varepsilon(t)$ for the January 22-29, 1974 storm.

Figure 3b Correlation between the AE index and the B_z component of the IMF for the January 22-29 storm; for details, see the caption for Figure 1a.

Figure 4a — The magnetic field $|B|$ and B_z and the combined auroral zone magnetic record (AE*) and the combined low latitude magnetic record (ASY*) for the storm of February 7-9, 1967.

Figure 4b — Comparison of the interplanetary quantities $|B|$, B_z, $\Sigma B_s \tau$, $V \times B_z$ (westward component only) and the magnetospheric quantities AE, Dst, ASY, AL for the storm of February 7-9, 1967.

Figure 4c — Comparison of the interplanetary quantities ε and the energy dissipated in the magnetosphere which includes both the joule heat dissipation and the ring current injection.

Figures 5a-g — DMSP photograph of the antarctic oval on June 12, 1975 and the simultaneous all-sky photograph taken from the South Pole: A dot with an arrow in the DMSP photograph indicates the location of South Pole. In the all-sky photograph, a white bar indicates an approximate location of the invariant pole. In the lower half of the figure, selected all-sky photographs from South Pole are shown, indicating changes of the auroras at about the time of the satellite passage.

Figure 6a A scatter plot of simultaneous measurements of the auroral kilometric radiation intensity (normalized to 30 R_E) and the auroral electrojet index AE using a random selection of 50 days of data from the IMP-6 spacecraft.

Figure 6b Simultaneous measurements of the auroral kilometric radiation intensity at 178 kHz by the IMP-6 satellite and the auroral electrojet index, AE, for a selection of days in which a close correlation is observed. The coordinates of IMP-6 are shown at the bottom of each panel.

Figure 7 Comparison of the observed north-south component electric field by the Chatanika radar and the inferred north-south electric field from the east-west auroral motions. If auroral motions would arise from the ionospheric electric field, all points should align along the line bisecting the first and fourth quadrants.

AFGL-TR-78-0269

INVESTIGATION OF THE PHENOMENOLOGY OF THE ARCTIC IONOSPHERE AND ITS RELATION TO THE PHENOMENOLOGY OF ARCTIC PRECIPITATION

S.-I. Akasofu

Geophysical Institute
University of Alaska
Fairbanks, Alaska 99701

Final Report
October 2, 1975 - September 30, 1978

PART II

September, 1978

Approved for public release; distribution unlimited

AIR FORCE GEOPHYSICS LABORATORY
AIR FORCE SYSTEMS COMMAND
ELECTRONIC SYSTEMS DIVISION
HANSCOM AFB, MASSACHUSETTS 01731

INTERPLANETARY ENERGY FLUX ASSOCIATED WITH MAGNETOSPHERIC SUBSTORMS

S.-I. Akasofu
Geophysical Institute
University of Alaska
Fairbanks, Alaska 99701

Abstract

In Part II, our new finding of the relationship between $\varepsilon(t)$ and the AE index will be described in more detail. In particular, it is shown that the interplanetary quantity $\varepsilon(t)$, obtained by Perreault and Akasofu (1978), for intense geomagnetic storms, also correlates well with individual magnetospheric substorms. This quantity is given by $\varepsilon(t) = V|B|^2 \sin^4 (\theta/2)\, \ell_0^{\,2}$, where V and $|B|$ denote the solar wind speed and the magnitude of the interplanetary magnetic field (IMF), respectively, and θ denotes the polar angle of the IMF; ℓ_0 is a constant $\approx$ 7 earth radii. The AE index is used in this correlation study. The correlation is good enough to predict both the occurrence and intensity of magnetospheric substorms observed in the auroral zone, by monitoring the quantity $\varepsilon(t)$ upstream of the solar wind.

1. Introduction

A number of studies have been made in the past in an attempt to find interplanetary quantities which are related to magnetospheric substorm activity. Snyder, Neugebauer and Rao (1963) and Olbert (1968) found a good correlation between the daily sum of the Kp index (denoted by ΣKp) and the solar wind speed. It is given by

$$V(\text{km/sec}) = 6.3\ \Sigma Kp + 262.$$

Ballif, Jones and Coleman (1969) showed that the variance of the interplanetary magnetic field is correlated with the Kp index. Fairfield and Cahill (1966) and Rostoker and Fälthammar (1967) were the first to recognize the importance of the B_z component of the interplanetary magnetic field (IMF) on the occurrence of magnetospheric substorms. Since then a large number of papers have been published, reporting a good correlation between the southward component of B_z (or $B_z < 0$) and the magnetospheric substorm index AE (cf. Arnoldy, 1971; Burton et al, 1975; for reviews, see Burch, J.L., 1974; Akasofu, 1977).

Most recently, however, Perreault (1974), Burlaga and Lepping (1977) and Perreault and Akasofu (1978) have examined closely this correlation and have found that the dependence of substorm activity on the B_z component is far from satisfactory. Burlaga and Lepping (1977) pointed out the importance of the solar wind speed in the correlation, in particular in a later period of recurrent geomagnetic storms. Perreault (1974) and Perreault and Akasofu (1978) noted that a significant substorm activity can occur even when the B_z component is positive and thus that

the magnetosphere cannot be a rectifier which passes only negative values of the B_z component. They found also that the magnitude of the B_z component alone cannot predict quantitatively the intensity of magnetospheric substorms and storms.

In their search for interplanetary quantities which can provide a better, quantitative correlation with substorm activity, they found the quantity $\varepsilon(t)$ given by

$$\varepsilon(t) = V|B|^2 \sin^4 \frac{\theta}{2} \, \ell_o^2$$

where

V = the solar wind speed

$|B|$ = the magnitude of the IMF

θ = the polar angle of the IMF vector in the y-z plane in solar-magnetospheric coordinates

$= \tan^{-1} (|B_y|/B_z)$ for $B_z > 0$

$= \pi - \tan^{-1} (|B_y|/B_z)$ for $B_z < 0$

ℓ_o = 7 earth radii.

The correlation between $\varepsilon(t)$ and the total energy $U(t)$ generated in the magnetosphere during twelve major geomagnetic storms is found to be quite good. The total dissipated energy U includes the ring current energy, joule heat energy associated with the auroral electrojet and the kinetic energy deposited in the polar ionosphere by auroral particles.

However, since all the major geomagnetic storms represent periods during which intense substorms occur very frequently, it was not possible for Perreault and Akasofu (1978) to examine in detail the relationship between $\varepsilon(t)$ and individual substorms.

The purpose of this paper is to examine the relationship between $\varepsilon(t)$ and the AE index for weak storms during which individual substorms can reasonably be resolved. Fortunately, the necessary interplanetary quantities in estimating $\varepsilon(t)$ are available for some of the recurrent geomagnetic storms in the interval 1973-1975. All quantities dealt with in this paper are hourly average values.

2. Results

(a) The November 3-10, 1973 Storm

This particular storm was examined by Burlaga and Lepping who noted that a good quantitative correlation between the B_z component and the AE index holds only during an initial period of recurrent storms and that the solar wind speed plays an important role in a later period.

In Figure 1a, the relationship between the AE index and the B_z component is shown for this particular storm. The B_z component was plotted in reverse; a negative period is hatched and a positive period is plotted by a dotted line. Further, the two quantities are normalized in such a way that peaks of both quantities have similar 'heights' during an initial period of the storm. As recognized correctly by Burlaga and Lepping (1977), a good correlation breaks down after the second day of the recurrent storm.

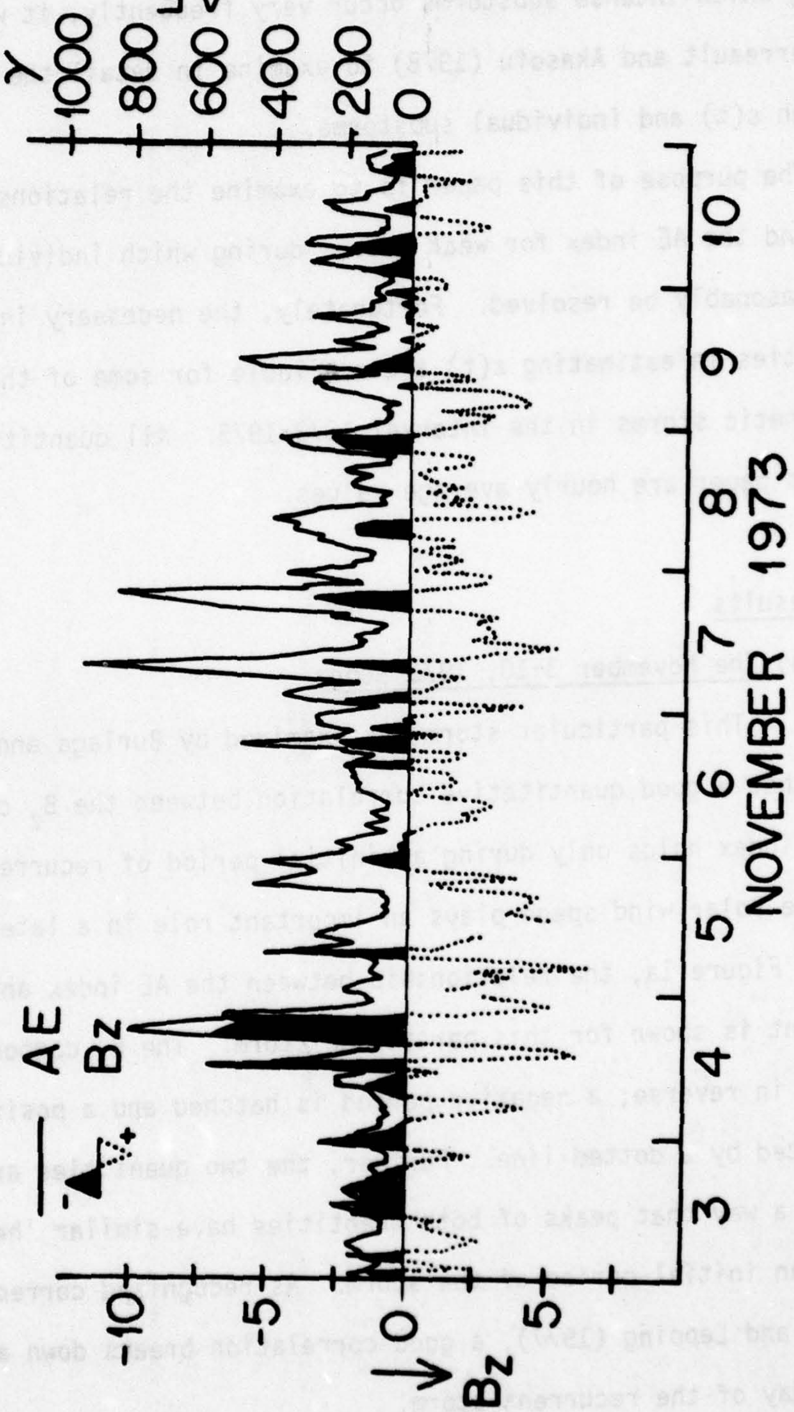
AE
Bz
1000
800
600
400
200
0
AE
10
-5
0
5
Bz
3
4
5
6
7
8
9
10
NOVEMBER 1973

Fig 1a

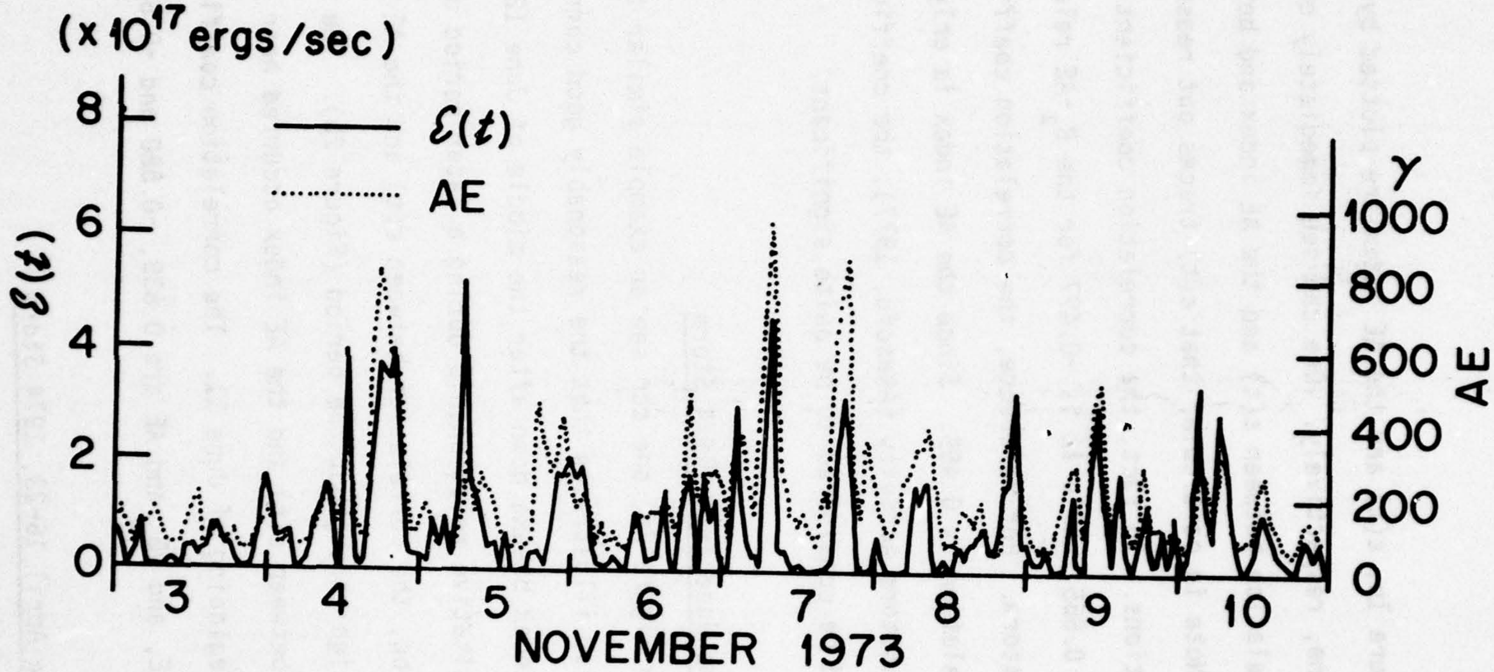

Fig 1b

In Figure 1b, $\varepsilon(t)$ and the AE index are plotted by a solid line and a dotted line, respectively. One can see immediately considerably higher correlation between $\varepsilon(t)$ and the AE index and between B_z and the AE index. Note in particular that $\varepsilon(t)$ traces out reasonably well AE index variations. In fact, the correlation coefficient for the $\varepsilon(t)$-AE relation is 0.665, while it is -0.477 for the B_z-AE relation for this particular storm. For reference, the correlation coefficient for the VB_z-AE correlation is 0.459. Since the AE index is only a rough index for substorm activity (Akasofu, 1977), the coefficient value of 0.665 should be considered to be quite significant.

(b) <u>The June 7-14, 1974 Storm</u>

In Figure 2a, one can see an example similar to (a). Figure 2a also illustrates that the reasonably good correlation between B_z and the AE index breaks down after the middle of June 12 and there is little quantitative relationship during a later period of the storm. On the other hand, the correlation between $\varepsilon(t)$ and the AE index remains remarkably high throughout the period (Figure 2b). The only serious discrepancy between $\varepsilon(t)$ and the AE index occurred near the end of June 10 and the beginning of June 11. The correlation coefficients between $\varepsilon(t)$ and AE, B_z and AE, and VB_z and AE are 0.639, -0.580 and -0.609, respectively.

(c) <u>The April 16-23, 1974 Storm</u>

This is another good example to show the breakdown of a good correlation between B_z and AE during a later period of a storm (Figure 3a). The correlation coefficient between B_z and AE is only -0.352. On

the other hand, the correlation between $\varepsilon(t)$ and AE is 0.565, much higher than the former value. For reference, the correlation coefficient between VB_z and AE is -0.447 for this particular storm. One should note also that in this particular storm the correlation between $\varepsilon(t)$ and AE become less than satisfactory during a later period of the storm.

(d) The January 22-29, 1974 Storm

This particular example provides an additional feature which is not apparent in the earlier ones. Again, one can easily recognize that the good correlation between B_z and AE lasted for less than one day and there is little quantitative relation during the rest of the storm (Figure 4a). The correlation coefficient between B_z and AE is only -0.367. The correlation between $\varepsilon(t)$ and AE is significantly higher, 0.562, than the former value.

However, in spite of a generally good correlation, one serious breakdown occurred on January 25 during which $\varepsilon(t)$ was considerably greater than what is predicted by the correlation with AE. This storm is quite unique, compared with the earlier examples, in that a significant main phase (-65 γ) developed on this day. It appears that the excess energy flux was deposited in the ring current belt. We shall discuss this feature later.

(e) The July 3-10, 1974 Storm

This storm is similar to the previous example in that a large excess of $\varepsilon(t)$ over AE occurred during the storm. Again, the correlation between B_z and AE is poor except for the first three days (Figure 5a), while the correlation between $\varepsilon(t)$ and AE is reasonably good for the

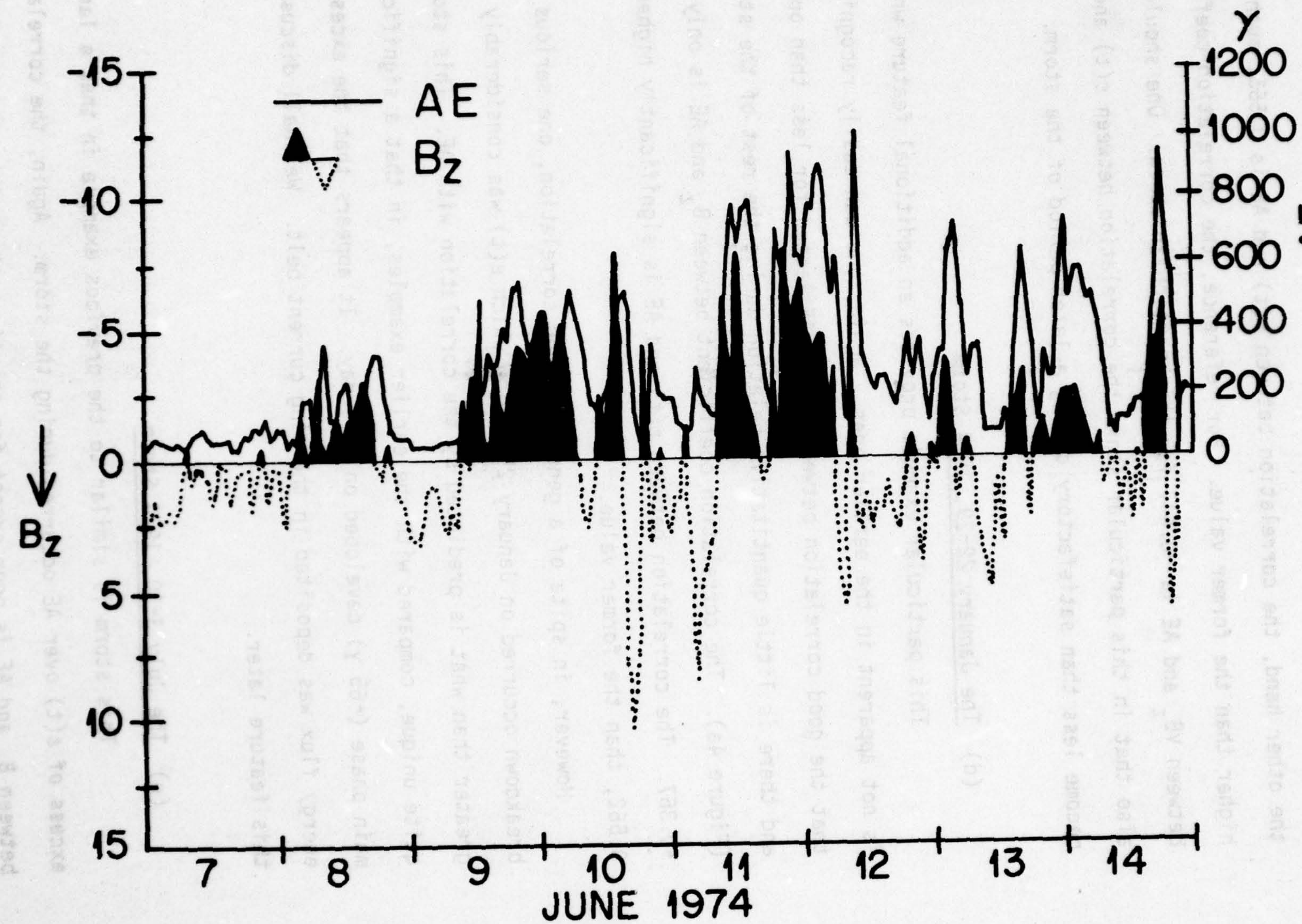
AE
B_z
-15
-10
-5
0
5
10
15
B_z
γ
1200
1000
800
600
400
200
0
AE
7
8
9
10
11
12
13
14
JUNE 1974

Fig 2a

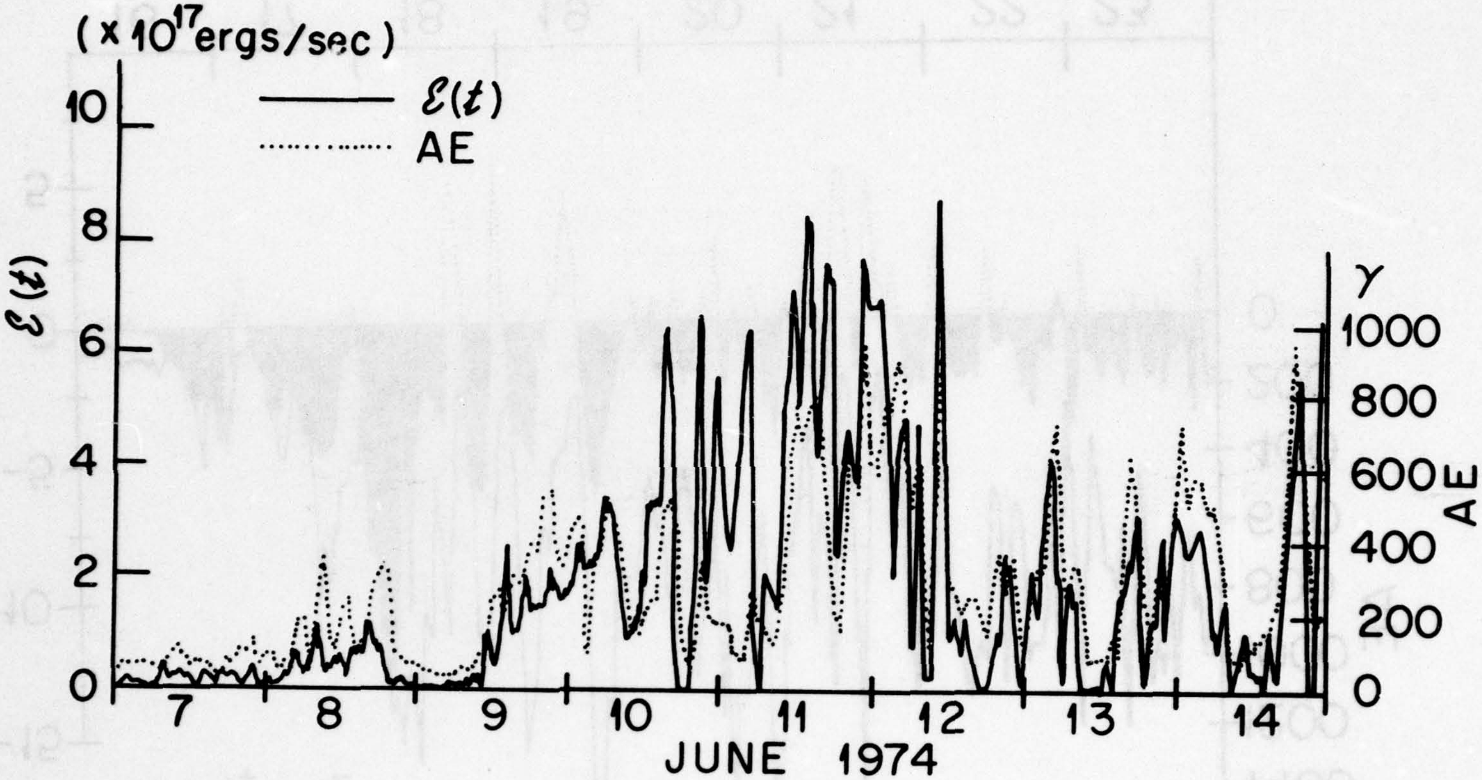

(x 10^{17} ergs/sec)
$\mathcal{E}(t)$
AE
10
8
6
4
2
0
γ
1000
800
600
400
200
0
AE
7
8
9
10
11
12
13
14
JUNE 1974

Fig 2b

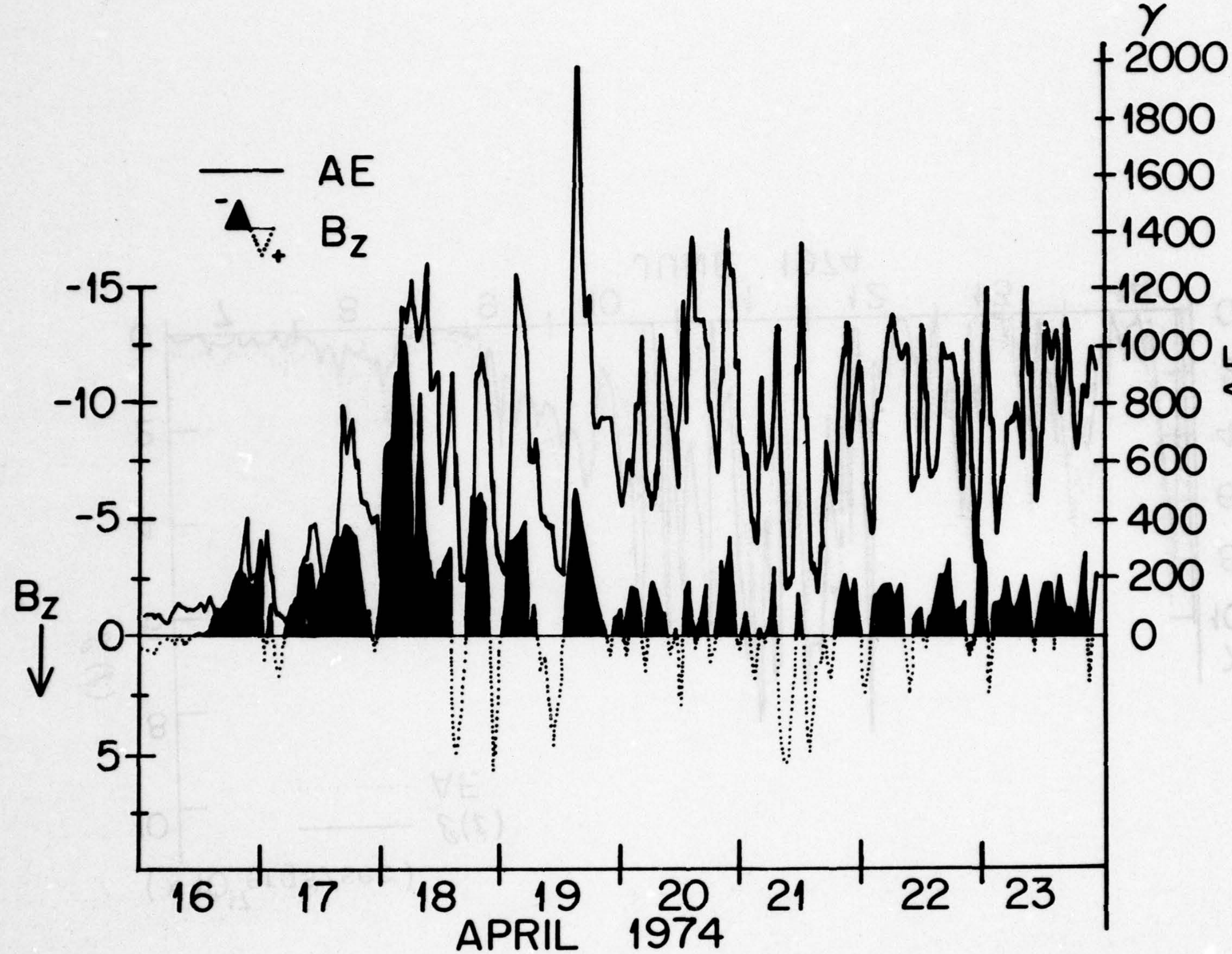
AE
B_z
-15
-10
-5
0
5
B_z
γ
2000
1800
1600
1400
1200
1000
800
600
400
200
0
AE
16
17
18
19
20
21
22
23
APRIL 1974

Fig 3a

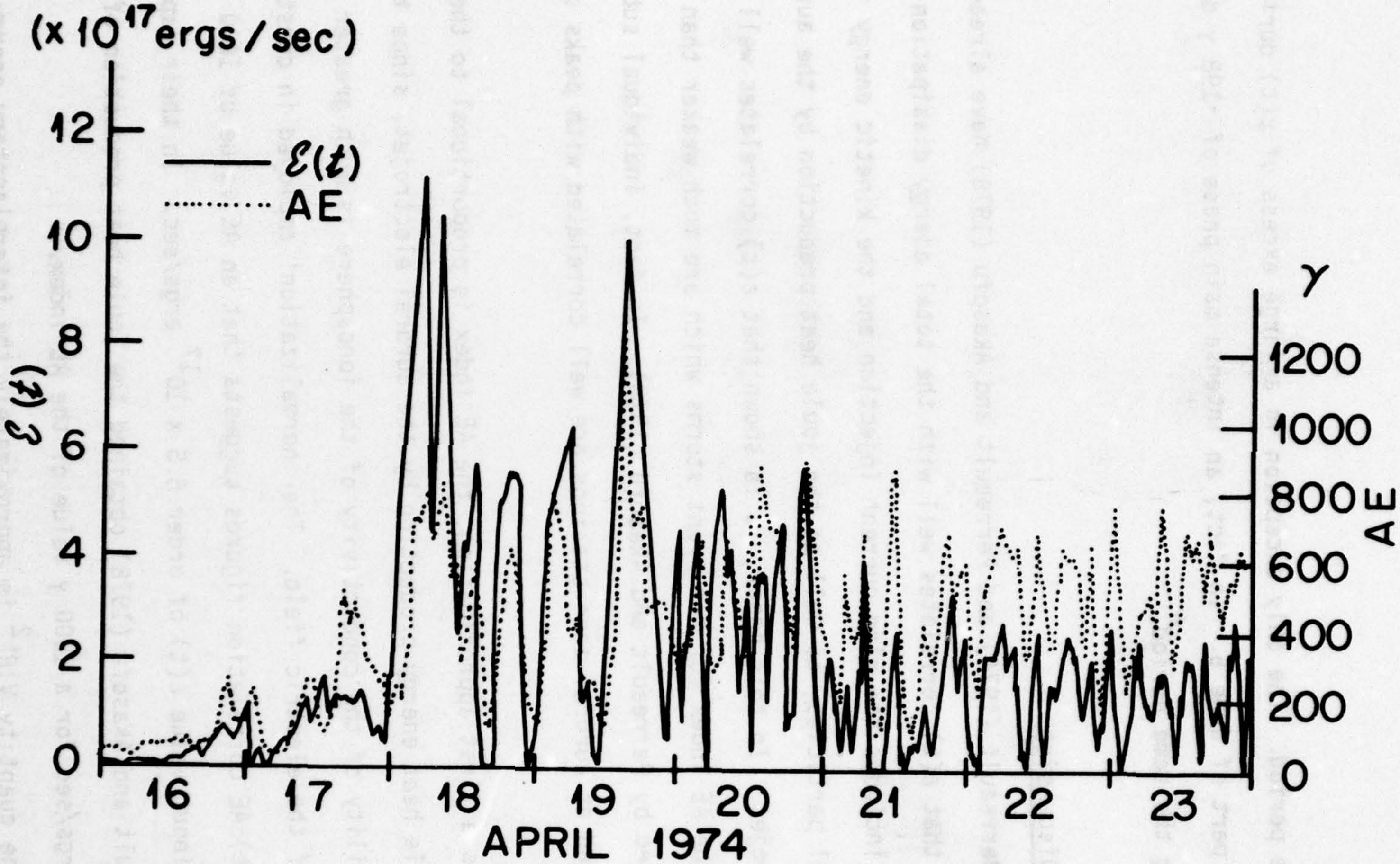
(x 10^17 ergs / sec)
ℰ(t)
ℰ(t)
AE
12
10
8
6
4
2
0
γ
1200
1000
800
600
400
200
0
AE
16
17
18
19
20
21
22
23
APRIL 1974

Fig 3b

entire period. The only exception is a large excess of $\varepsilon(t)$ during an early part of June 6. In fact, an intense main phase of -198 γ developed during the same period.

3. Discussion

Perreault (1974) and Perreault and Akasofu (1978) have already shown that $\varepsilon(t)$ correlates well with the total energy dissipation U which includes the ring current injection and the kinetic energy flux of auroral particles, as well as the joule heat production by the auroral electrojet. In this paper, it is shown that $\varepsilon(t)$ correlates well also with the AE index for recurrent storms which are much weaker than those examined by Perreault and Akasofu (1978). In fact, individual substorms observed at auroral zone stations are well correlated with peaks of $\varepsilon(t)$.

As a first approximation, the AE index is proportional to the rate of joule heat energy production by the auroral electrojet, since the variability of the conductivity of the ionosphere is much greater than that of the electric field. The 'normalization' employed in constructing the $\varepsilon(t)$-AE correlation figures suggests that an AE value of 1000 γ corresponds to an input value $\varepsilon(t)$ of order 6.5×10^{17} ergs/sec. In their paper, Perreault and Akasofu (1978) obtained the joule heat production of 5.5×10^{17} ergs/sec for a 1000 γ value of the AE index.

The quantity $V|B|^2$ is approximately the interplanetary energy flux per unit area and $(\ell_0 \sin^2(\theta/2))^2$ may be considered to be the cross-section through which the energy flux flows into the magnetosphere. It is interesting to note that V and $|B|$ vary much more smoothly than $\sin^4(\theta/2)$. Thus, the term $\sin^4(\theta/2)$ tends to construct individual substorms. However, all the

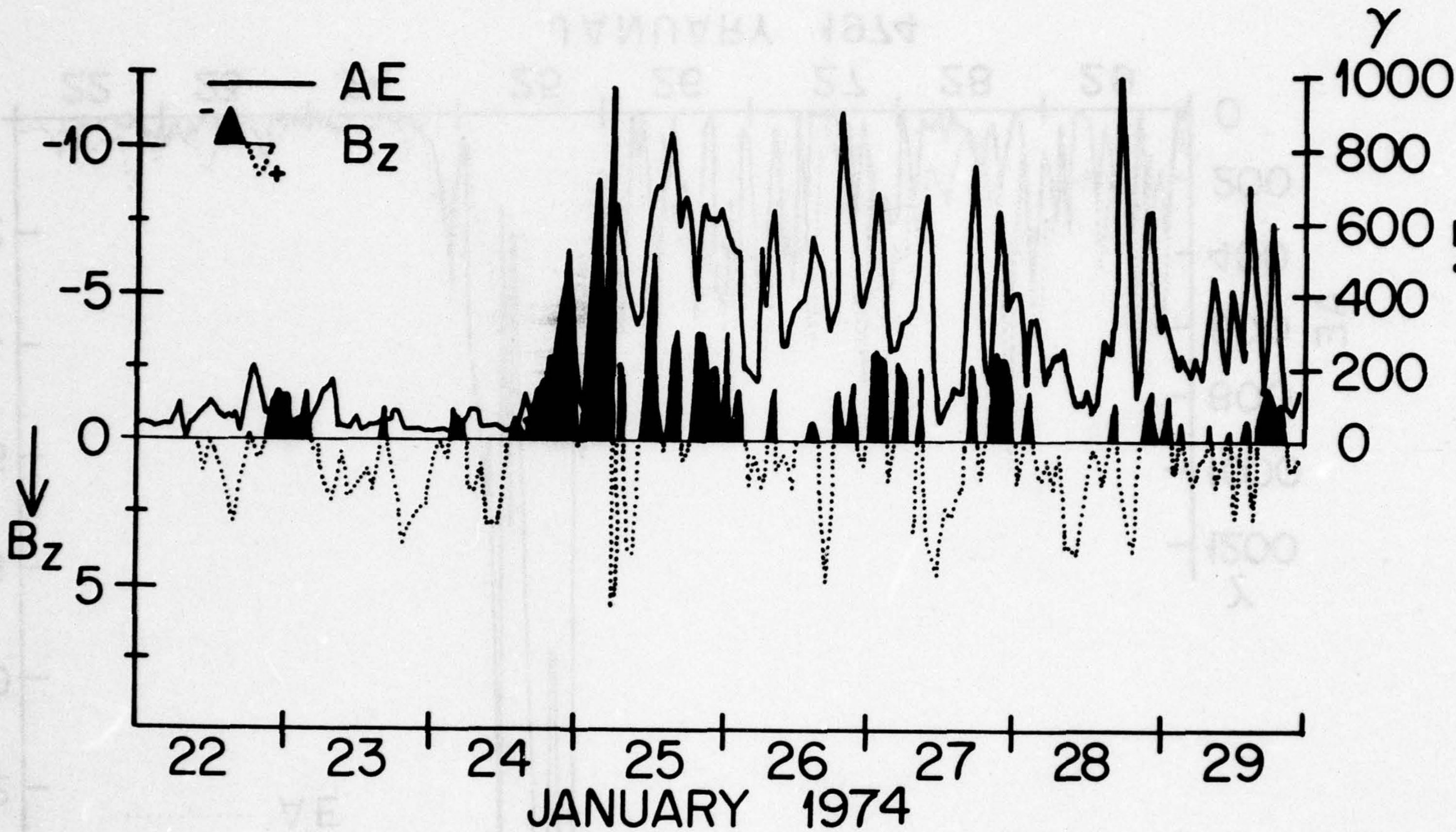
AE
B_z
-10
-5
0
5
B_z
γ
1000
800
600
400
200
0
AE
22
23
24
25
26
27
28
29
JANUARY 1974

Fig 4a

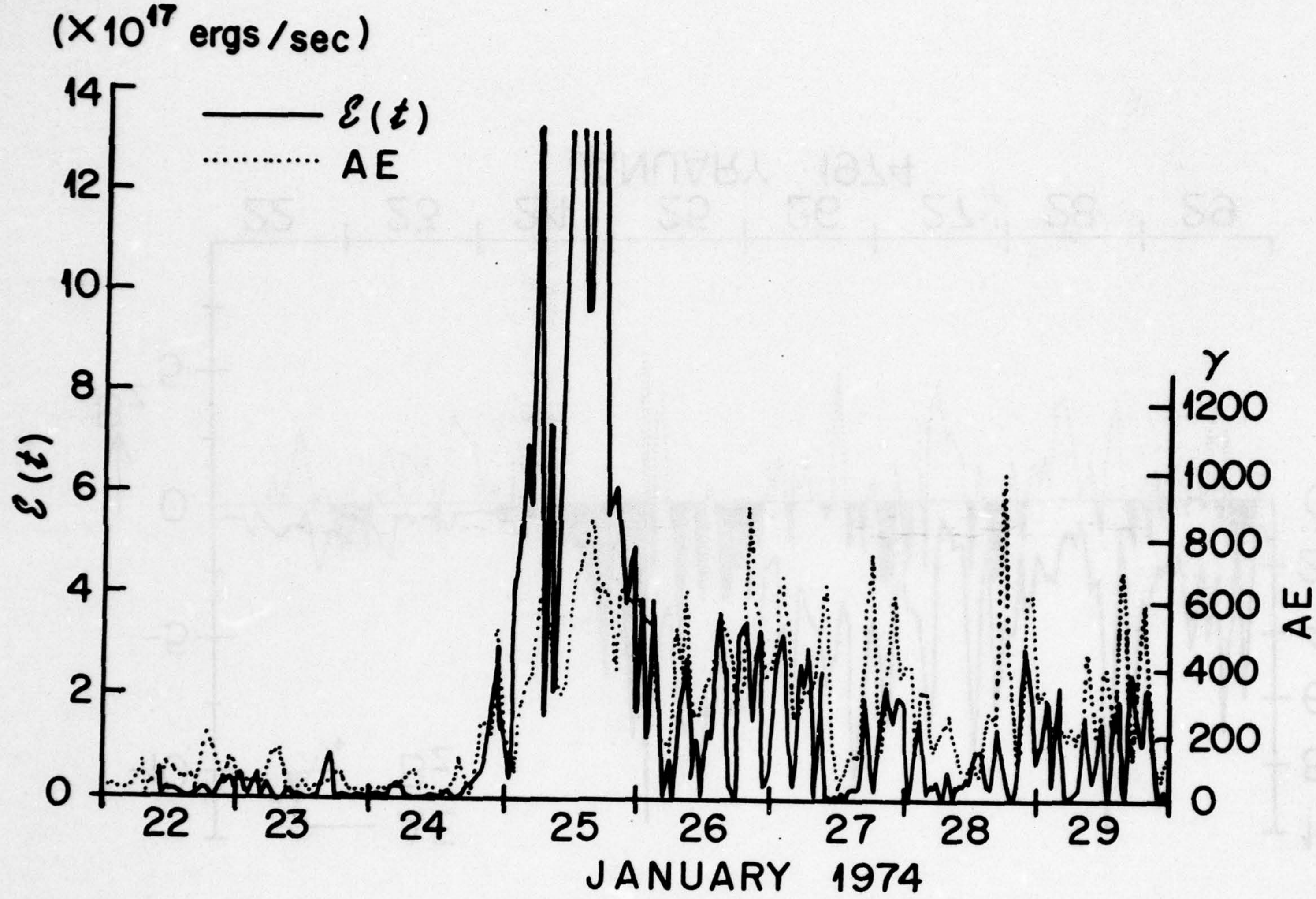
(×10^17 ergs/sec)
$\mathcal{E}(t)$
AE
14
12
10
8
6
4
2
0
γ
1200
1000
800
600
400
200
0
AE
22
23
24
25
26
27
28
29
JANUARY 1974

Fig 4b

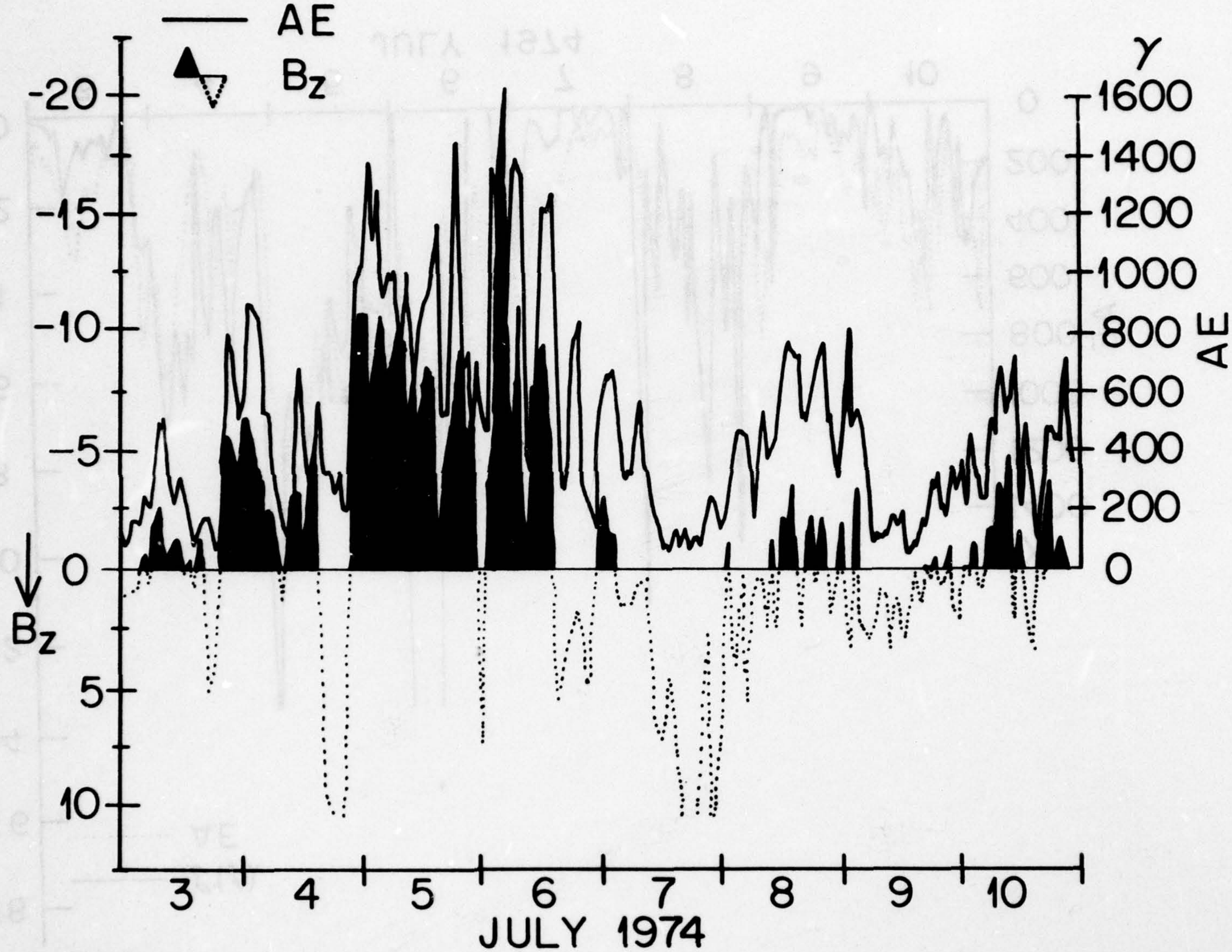
AE
B_z
-20
-15
-10
-5
0
5
10
B_z
γ
1600
1400
1200
1000
800
600
400
200
0
AE
3
4
5
6
7
8
9
10
JULY 1974

Fig 5a

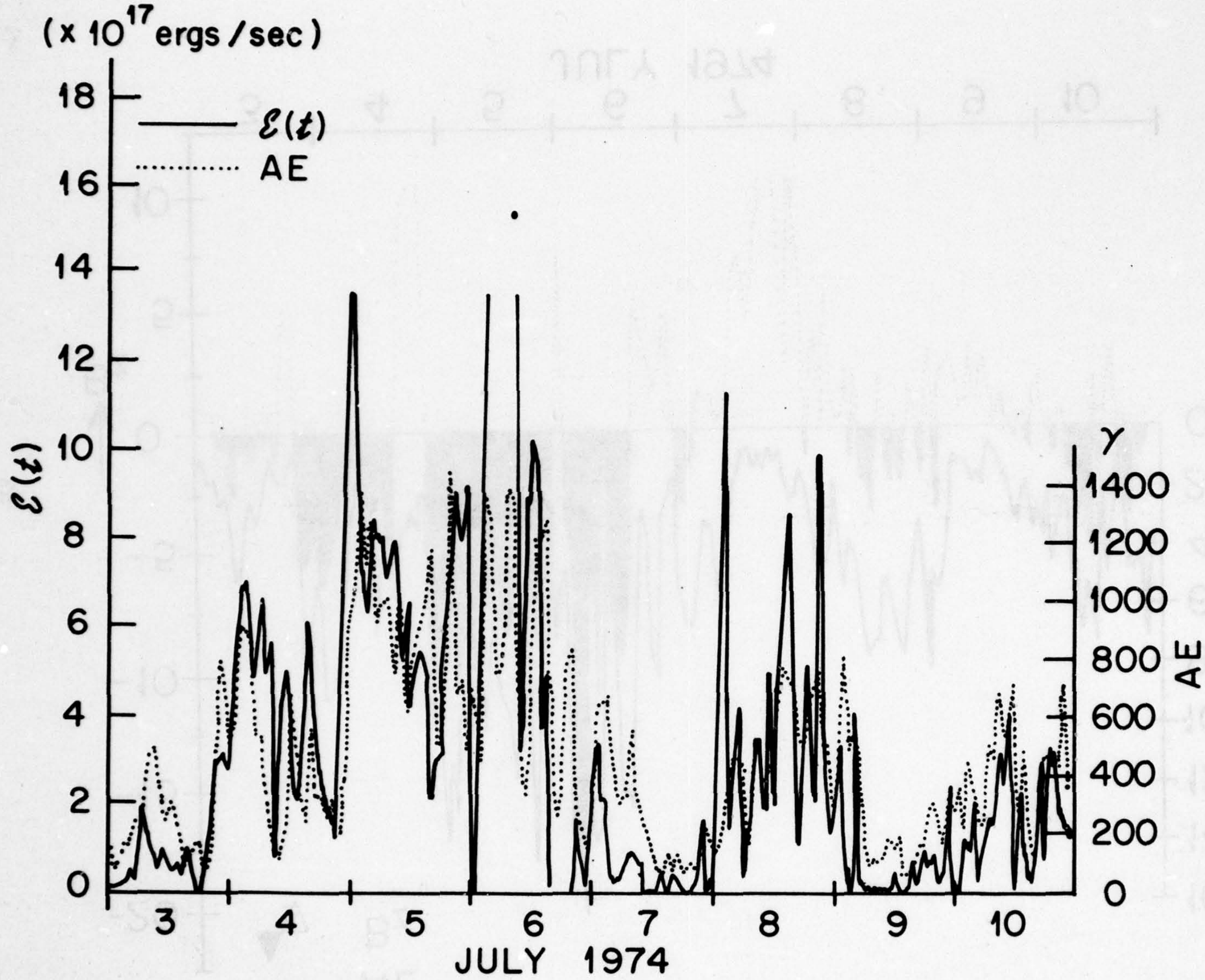
(x 10^17 ergs / sec)
ℰ(t)
AE
ℰ(t)
0
2
4
6
8
10
12
14
16
18
Y
AE
0
200
400
600
800
1000
1200
1400
3
4
5
6
7
8
9
10
JULY 1974

Fig 5b

three parameters, V, $|B|$ and $\sin^4(\theta/2)$, contribute in determining the intensity of substorms observed at the standard auroral zone stations. It is also important to recognize that the correlation with the AE index is higher with $\varepsilon(t) = V|B|^2 \sin^4(\theta/2) \ell_0^2$ than with B_z or VB_z.

Recognizing that the AE index is only a rough index for magnetospheric substorm activity, the correlation coefficient between $\varepsilon(t)$ and AE of order 0.6 can be considered to be satisfactory. Indeed, it may be worthwhile to re-examine the AE index in some instances. In particular, since the AE index cannot properly reflect substorm activity along a contracted oval, the correlation refers only to substorms observed at the standard auroral zone stations.

It is also shown that when $\varepsilon(t)$ 'exceeds' greatly the energy dissipated in terms of the joule heat production in the ionosphere, a significant ring current develops in the magnetosphere. Indeed, it has been shown by a number of workers that the rate of energy injection in building up an appreciable ring current exceeds the rate of joule heat energy production (cf. Akasofu, 1977, p. 274).

4. Conclusion

With this success of obtaining a reasonable correlation between $\varepsilon(t)$ and AE, we should be able to predict both the occurrence and intensity of magnetospheric substorms, as well as the growth of the ring current, if the interplanetary quantities V, $|B|$, and θ can be monitored on a real time basis.

Acknowledgments. The author would like to thank Dr. P. Perreault for his discussion on the results reported in this paper. The project was supported in part by a grant from the National Science Foundation, Atmospheric Sciences Section ATM74-23832 and in part by AF Contract F19628-76-C-0074.

References

Akasofu, S.-I., Physics of Magnetospheric Substorms, D. Reidel Pub. Co., Dordrecht-Holland, 1977.

Ballif, J.R., D.E. Jones and P.J. Coleman, Jr., Further evidence on the correlation between transverse fluctuation in the interplanetary magnetic field and Kp., J. Geophys. Res., 74, 2289, 1969.

Burch, J.L. Observations of interactions between interplanetary and geomagnetic fields, Rev. Geophys. Space Phys., 12, 1969, 1974.

Burlaga, L.F. and R.P. Lepping, The causes of recurrent geomagnetic storms, Planet. Space Sci., 25, 1151, 1977.

Burton, R.K., R.L. McPherron and C.T. Russell, An empirical relationship between interplanetary conditions and Dst, J. Geophys. Res., 80, 4204, 1975.

Fairfield, D.H. and L.J. Cahill, Jr., Transition region magnetic field and polar magnetic disturbances, J. Geophys. Res., 71, 155, 1966.

Olbert, S. Summary of experimental results from M.I.T. detector on IMP-1, Physics of the Magnetosphere, (ed. by R.L. Carovillano, J.F. McClay and H.R. Radoski), P.641, D. Reidel Pub. Co., Dordrecht-Holland, 1968.

Perreault, P., On the relationship between interplanetary magnetic fields and magnetospheric storms and substorms, Ph.D. Thesis, Univ. Alaska, August, 1974.

Perreault, P. and S.-I. Akasofu, A study of geomagnetic storms, Geophys. J. Roy. Astron. Soc., 54, (in press), 1978.

Rostoker, G. and C.-G. Fälthammar, Relationship between changes in the interplanetary magnetic field and variations in the magnetic field at the earth's surface, J. Geophys. Res., 72, 5853, 1967.

Snyder, C.W., M. Neugebauer and U.R. Rao, The solar wind velocity and its correlation with cosmic-ray variations and with solar and geomagnetic activity, J. Geophys. Res., 68, 6361, 1963.

Figure Captions

Figure 1a Correlation between the auroral electrojet index AE and the B_z component of the interplanetary magnetic field (IMF) for the November 3-10, 1973 storm. The B_z component is plotted in reverse and negative periods are hatched; positive periods are plotted by a dotted line.

Figure 1b Correlation between the auroral electrojet index AE and the interplanetary quantity $\varepsilon(t)$ for the November 3-10, 1973 storm.

Figure 2a Correlation between the AE index and the B_z component of the IMF for the June 7-14, 1974 storm; for details see the caption for Figure 1a.

Figure 2b Correlation between the AE index and $\varepsilon(t)$ for the June 7-14, 1974 storm.

Figure 3a Correlation between the AE index and the B_z component of the IMF for the April 16-23, 1974 storm; for details, see the caption for Figure 1a.

Figure 3b Correlation between the AE index and $\varepsilon(t)$ for the April 16-23 storm.

Figure 4a Correlation between the AE index and the B_z component of the IMF for the January 22-29 storm; for details see the caption for Figure 1a.

Figure 4b Correlation between the AE index and $\varepsilon(t)$ for the January 22-29, 1974 storm.

Figure 5a Correlation between the AE index and the B_z component of the IMF for the July 3-10, 1974 storm; for details, see the caption for Figure 1a.

Figure 5b Correlation between the AE index and $\varepsilon(t)$ for the July 3-10, 1974 storm.